Near-term Effects of the Lower Atmosphere in Simulated Northwest Flow Snowfall Forced over the Southern Appalachians

UNIVERSITY *of* NORTH CAROLINA
ASHEVILLE

Douglas K. Miller
Associate Professor
Atmospheric Sciences Department
UNC Asheville
dmiller@unca.edu

Outline

- Introduction
- Methodology
- 6 – 8 December 2010 NWFS
- ARW-WRF simulations
  - Default
  - No surface sensible heat flux
  - No surface latent heat flux
- Summary and forecasting implications

Introduction

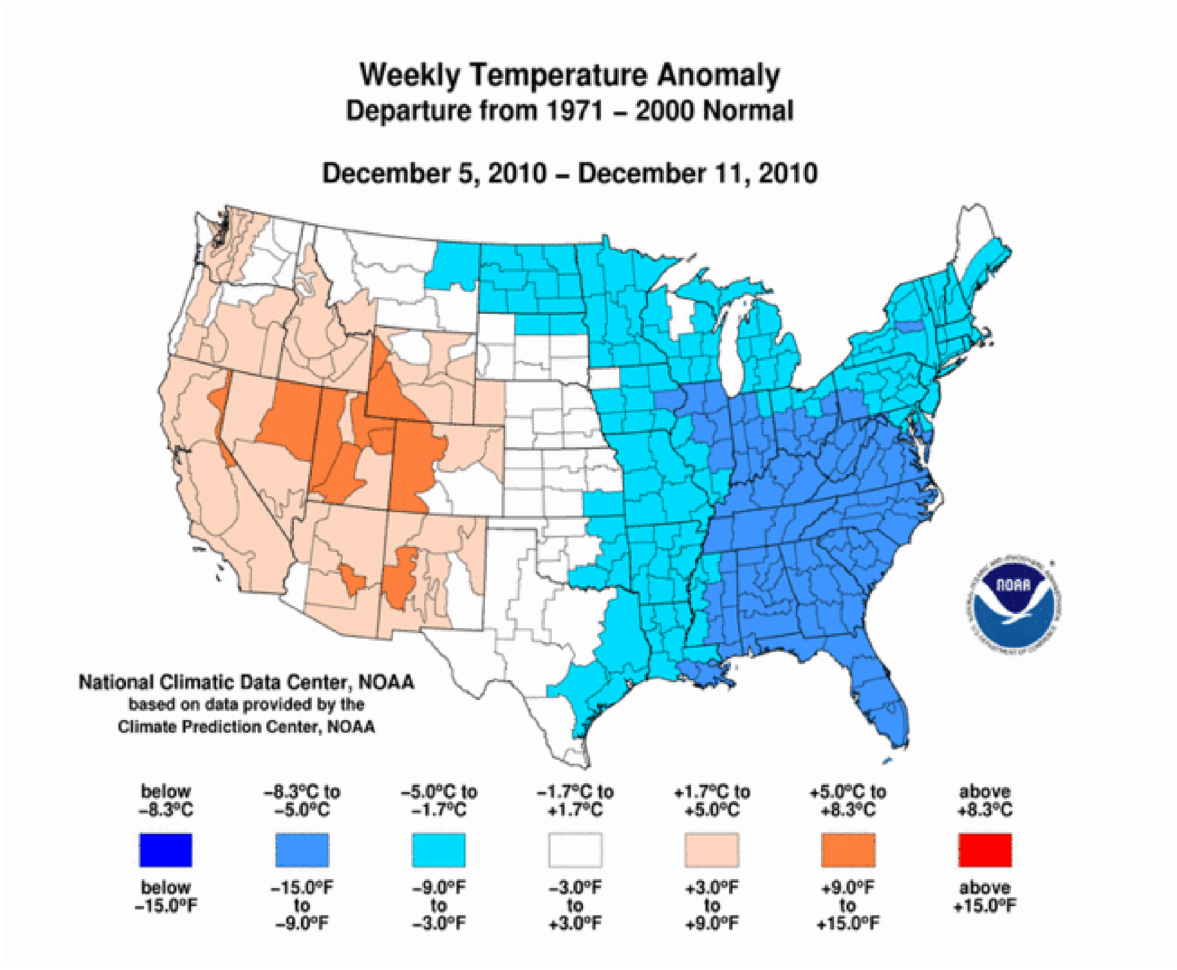

http://www1.ncdc.noaa.gov/pub/data/cmb/images/weekly/us/2010/tanom20101211-pg.gif

Introduction

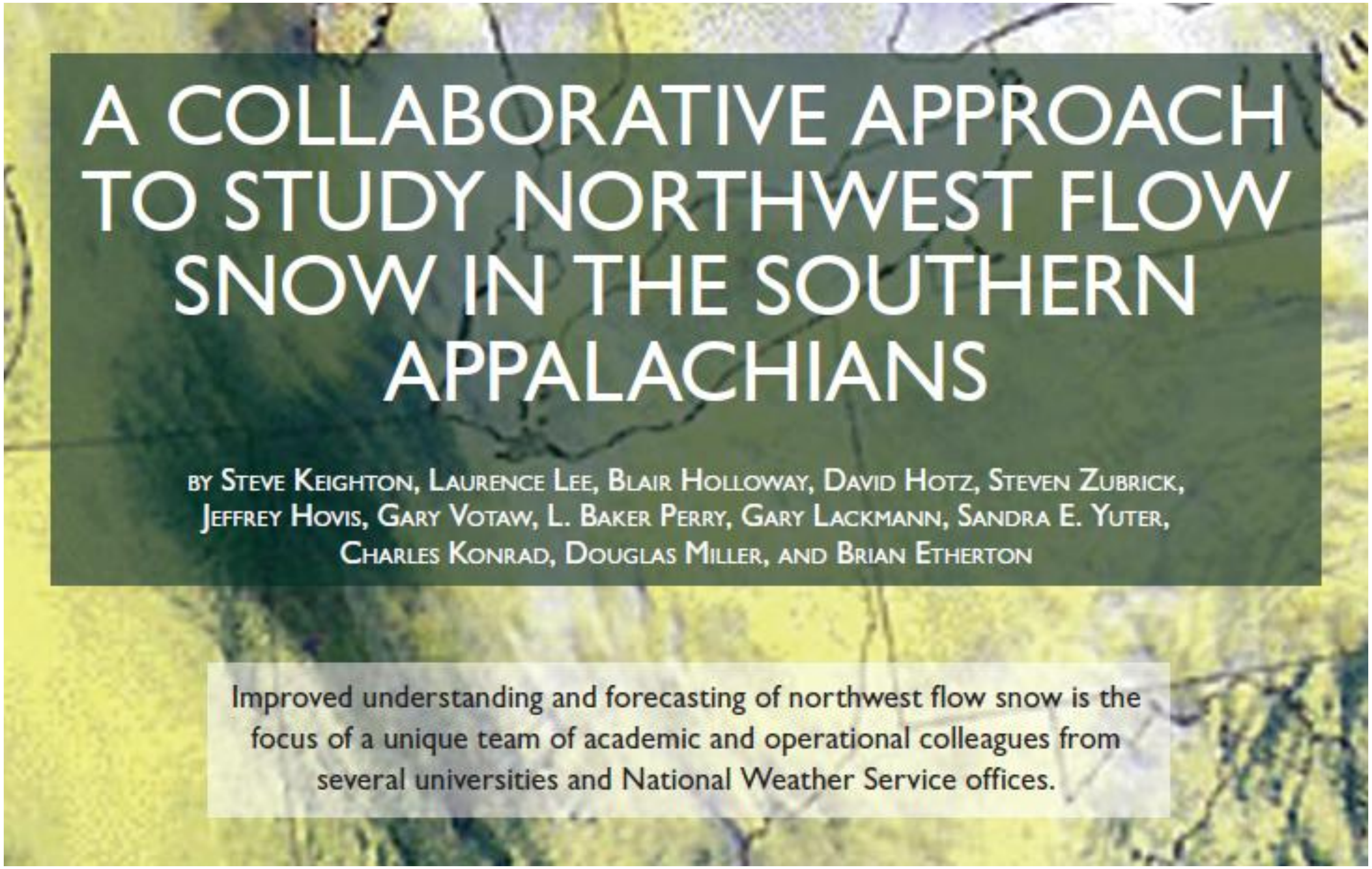
A COLLABORATIVE APPROACH TO STUDY NORTHWEST FLOW SNOW IN THE SOUTHERN APPALACHIANS

BY STEVE KEIGHTON, LAURENCE LEE, BLAIR HOLLOWAY, DAVID HOTZ, STEVEN ZUBRICK, JEFFREY HOVIS, GARY VOTAW, L. BAKER PERRY, GARY LACKMANN, SANDRA E. YUTER, CHARLES KONRAD, DOUGLAS MILLER, AND BRIAN ETHERTON

Improved understanding and forecasting of northwest flow snow is the focus of a unique team of academic and operational colleagues from several universities and National Weather Service offices.

Provides most of the background information on the current understanding of Northwest Flow Snowfall (NWFS) events

Introduction

- “Great Lakes Tap” with NWFS events
  - moistening
  - destabilization

  of lower layers

Introduction

- Surface effects closer to the southern Appalachians impacting NWFS events?
  - Mode of convection (diurnal cycle)
    - Ground as source/sink of heat
  - Reverse “seeder feeder” mechanism
    - Ground as source of ice nucleii
  - Moist soil conditions
    - Ground as source of water vapor

Introduction

- Purpose
  - to investigate the potential impact of antecedent surface conditions directly upstream of the Southern Appalachian Mountains (SAMs) through experiments using the ARW-WRF mesoscale model

Methodology

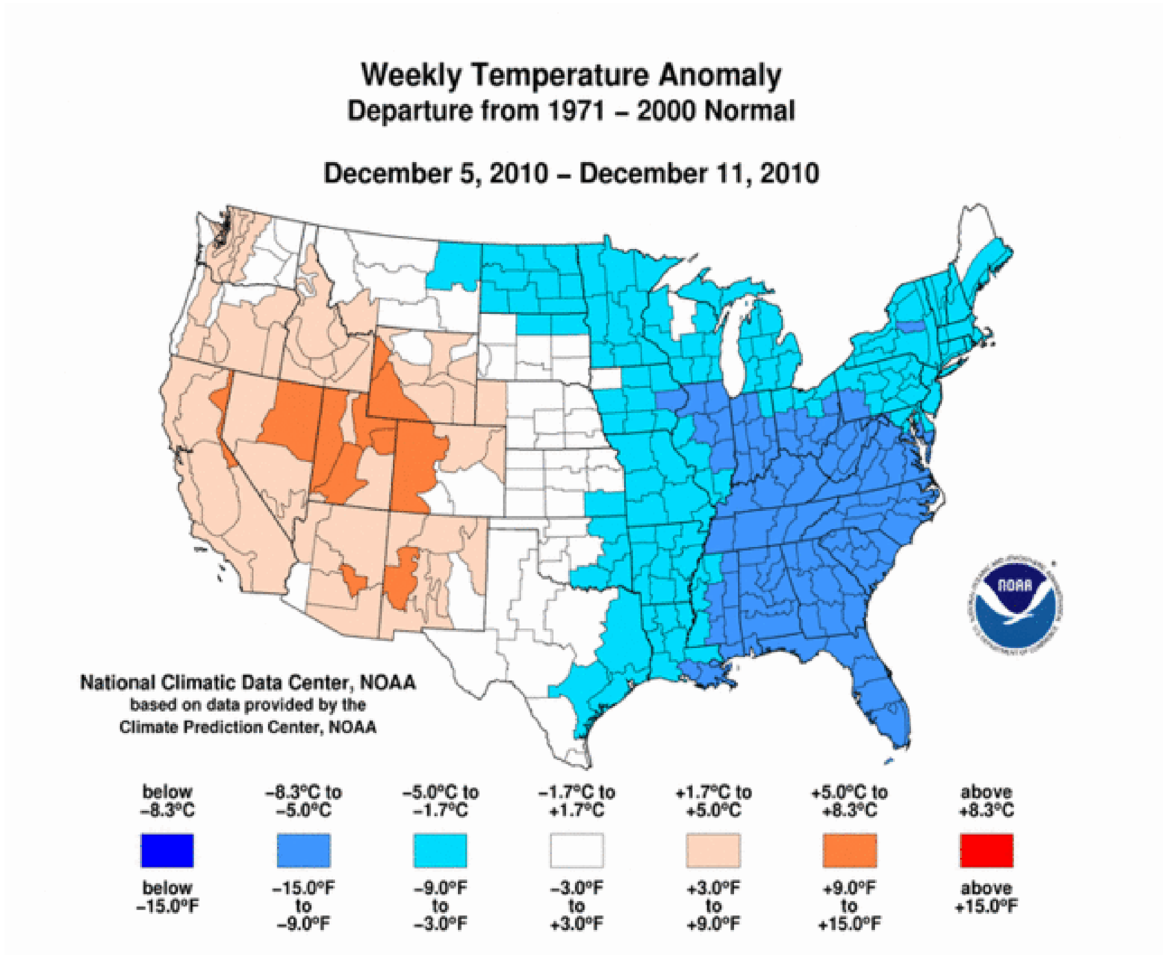

http://www1.ncdc.noaa.gov/pub/data/cmb/images/weekly/us/2010/tanom20101211-pg.gif

Methodology

- Version 3.1.1 of the ARW-WRF mesoscale model
- Four nested model domains centered on a point in the SAMs,
  - horizontal grid spacing varied in ratios of three from 13.5 km of the outermost nest down to 0.5 km of the innermost nest

Study domain

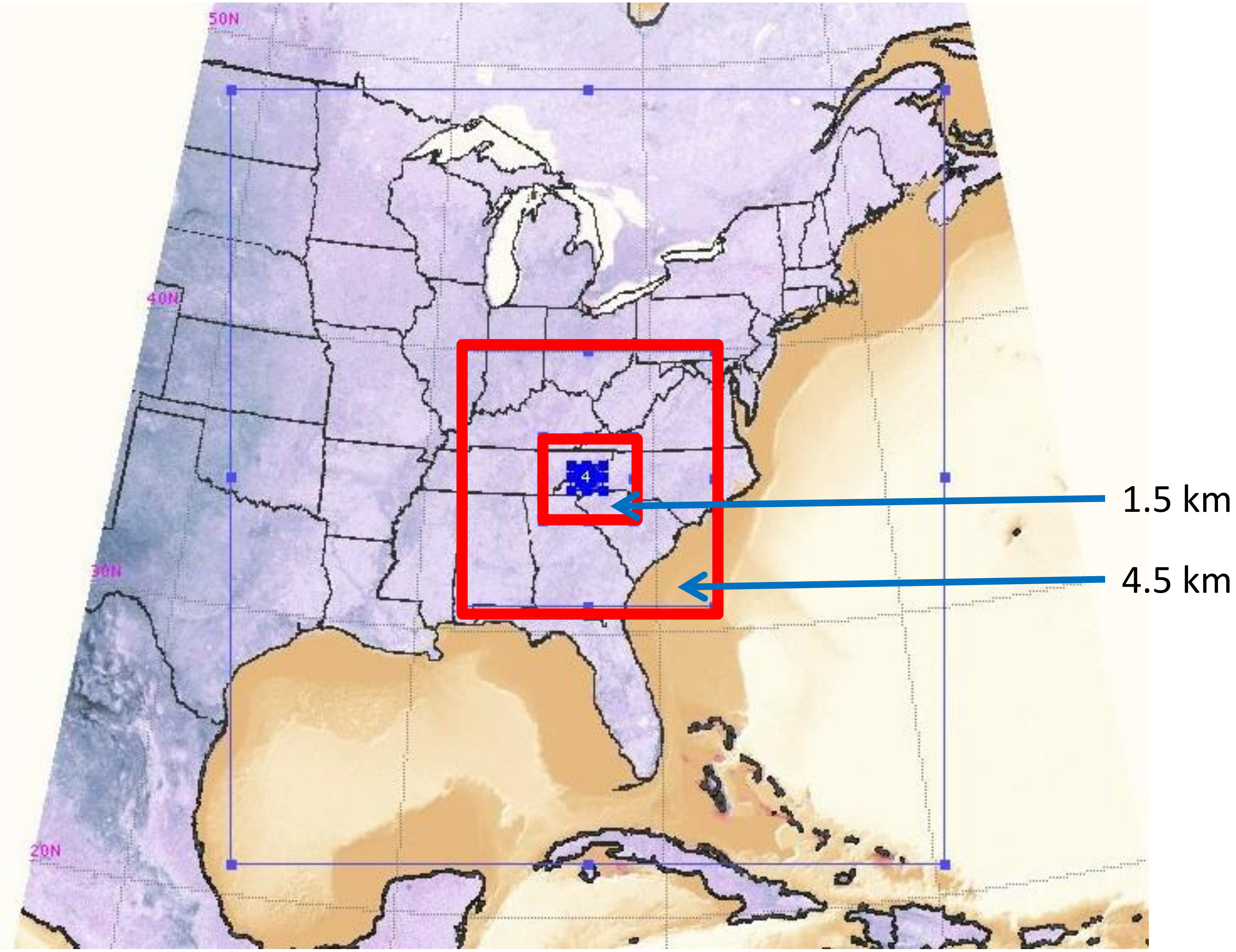

Study domain

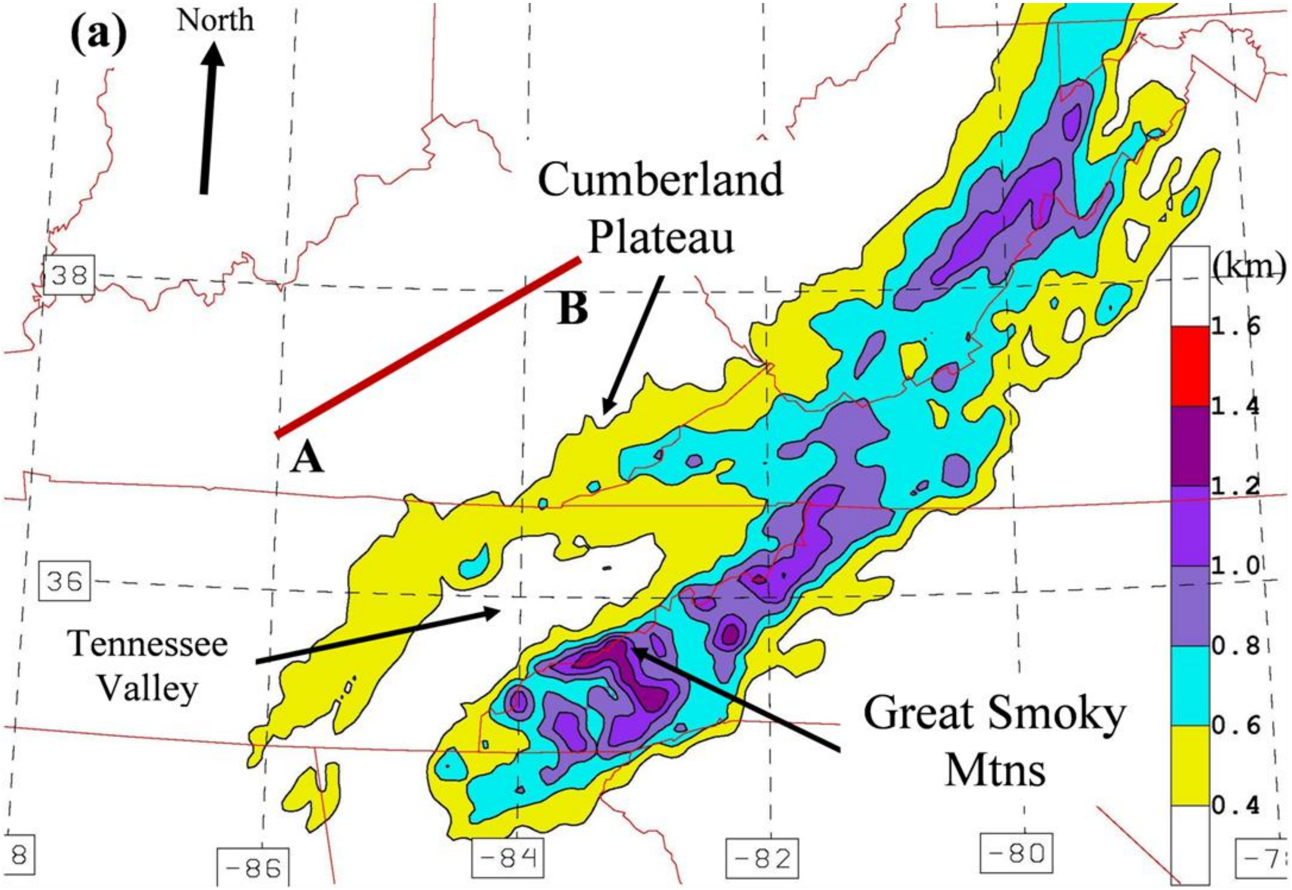

Nested domain 2 terrain elevation (km) exceeding 400 m above sea level. Line marked A-B is the orientation of the vertical cross section shown in later figures located upwind of the southern Appalachian Mountains.

Study domain

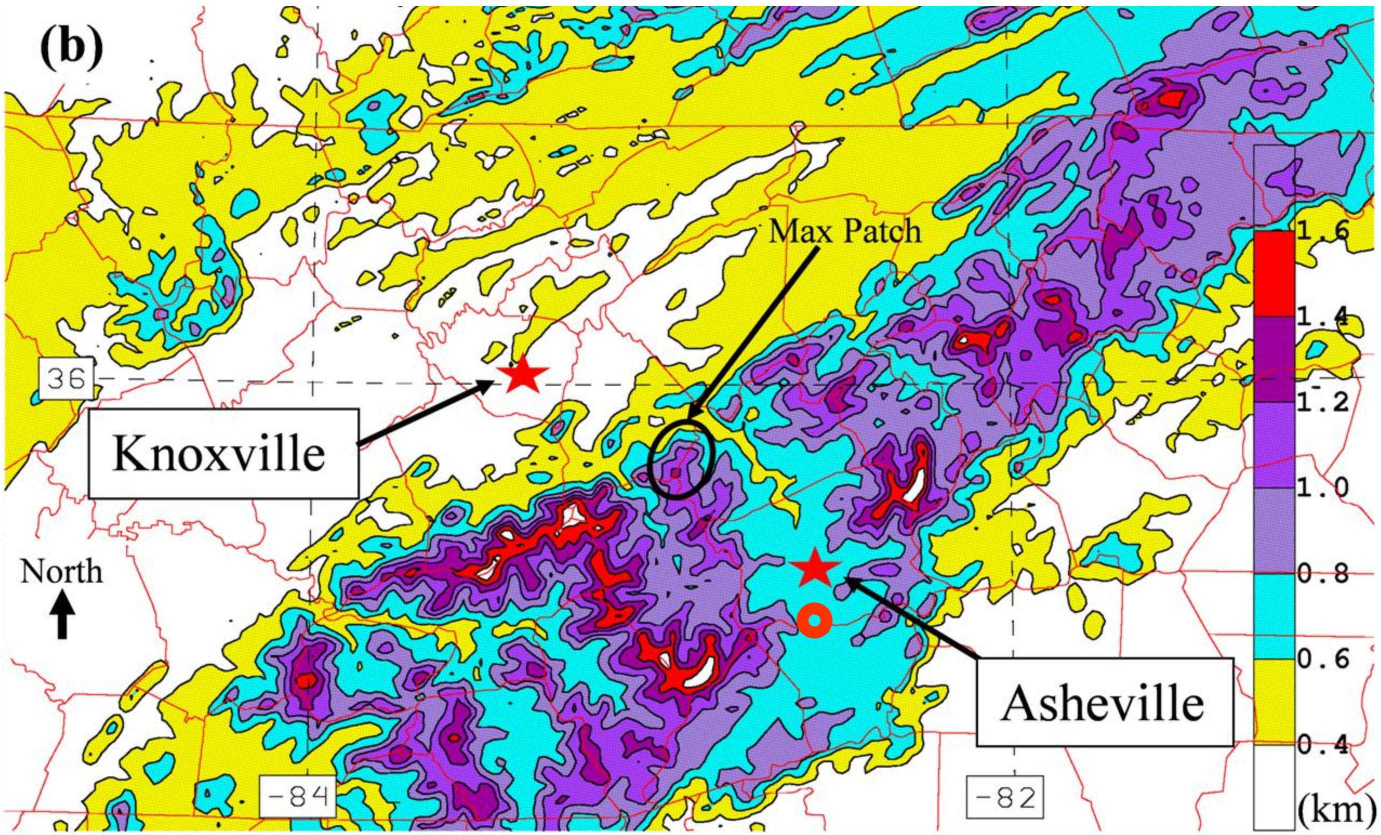

Nested domain 3 terrain elevation (km) exceeding 400 m above sea level. Locations of cities in the southern Appalachian Mountains are indicated in by the star symbol and the location of Max Patch is highlighted by the oval. Location of the KAVL ASOS is indicated by the open circle.

Methodology

- 45 model vertical levels extended from the ground to the model top at the 100 hPa level.
- one way nesting; simulated model fields on the innermost grids didn't feed back to fields on the outer nests.

Methodology

- Specified model physics
  - WRF single-moment 5-class microphysics (WSM5) explicit moisture scheme
  - Monin-Obukhov similarity theory-based surface layer scheme linked with
  - Yonsei University PBL scheme
  - unified Noah land-surface model with four soil layers

Methodology

- Specified model physics
  - Betts-Miller-Janjic convective parameterization scheme switched “on” for only the two outer domains (13.5 and 4.5 km domains)
  - Rapid Radiative Transfer Model (RRTM) longwave
  - Eta Geophysical Fluid Dynamics Laboratory shortwave radiation schemes

Methodology

- 48-h time integration
- initial conditions and lateral boundary conditions were derived from the NCEP-NCAR North American Regional Reanalysis surface and atmospheric fields
  - NOMADS web-access archive available at http://nomads.ncdc.noaa.gov/data.php .

Methodology

- The initial conditions were generated using the WRF Environmental Modeling System (EMS) Version 3.1 software
  - model start time at 0000 UTC 6 December 2010
  - lateral boundary conditions for the outermost domain were created via the WRF EMS software and updated <u>every six hours</u> up to and including the model simulation end time at 0000 UTC 8 December 2010 (Table 1).

Methodology

Period	**Designator**
0000 UTC 6 Dec – 1200 UTC 6 Dec 2010	P1
1200 UTC 6 Dec – 0000 UTC 7 Dec 2010	P2
0000 UTC 7 Dec – 0000 UTC 8 Dec 2010	P34

red = daylight hours

Methodology

- ARW-WRF model experiments
  - “SH off” or “LH off”
    - during the first 12-h period of the model simulation (P1),
    - during the middle 12-h period of the model simulation (P2), or
    - during the final 24-h period of the model simulation (P34).
  - The remainder of the model time integration consisted of using either the “default,” “50% SH enhancement,” or “50% LH enhancement” unified Noah land-surface model.

Methodology

- “Enhanced” experiments in this study
  - The enhanced experiments involved multiplying the “default” estimate by 1.5, changing the magnitude of the surface moisture or heat fluxes without modifying their direction
    - “What if” default land-surface model had a low flux magnitude (damped) bias due to
      - imperfect model physics (e.g., transfer coefficient underestimate)
      - poor surface moisture or temperature initialization.

Methodology

- The surface sensible and latent experiment simulations were run separately so that the impacts of surface warming and surface moistening could be assessed in a more straightforward manner.

6 – 8 December 2010
NWFS

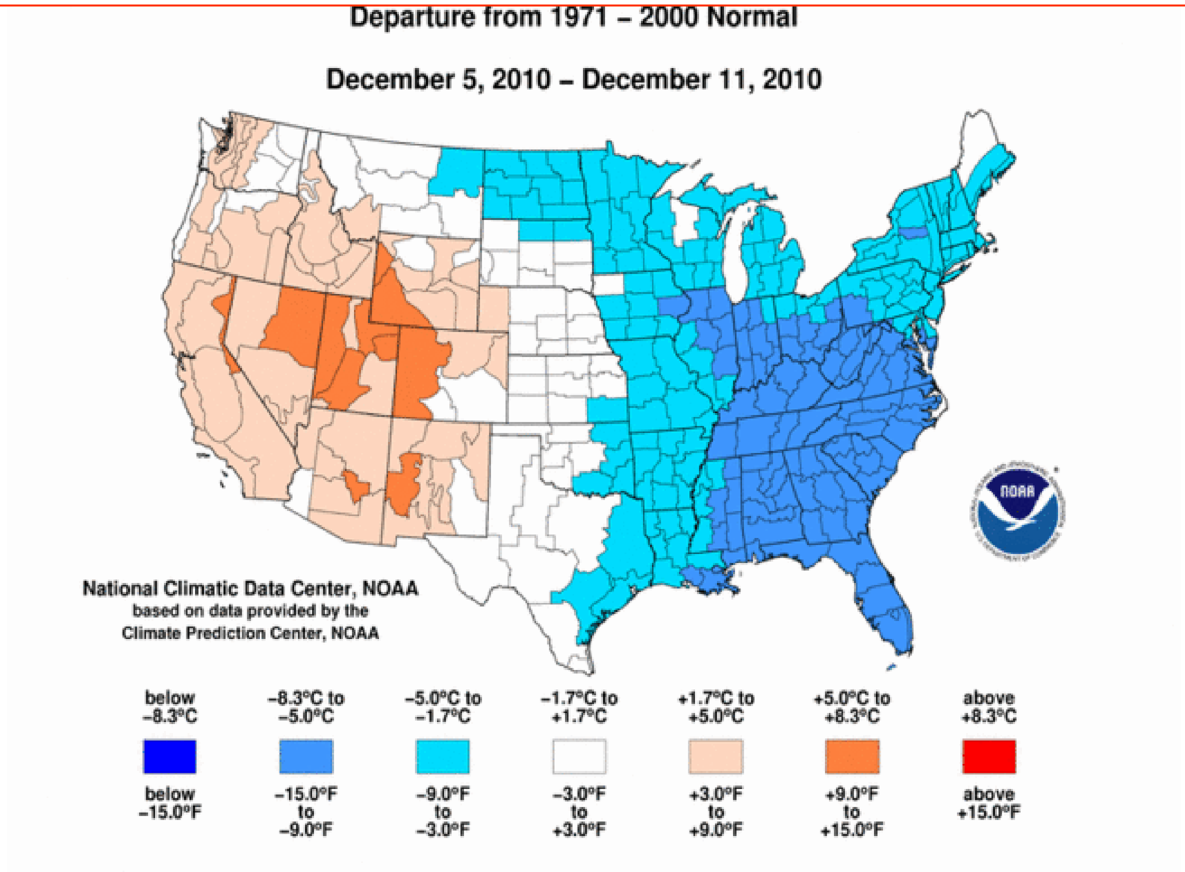

http://www1.ncdc.noaa.gov/pub/data/cmb/images/weekly/us/2010/tanom20101211-pg.gif

6 – 8 December 2010 NWFS

- Why 6 – 8 December 2010 case study?
  - It was the first NWFS event of moderate snow accumulation during the 2010-2011 cool season and was potentially driven, in part, by surface conditions in which the land surface over the central and eastern U.S. had not yet become “winterized” (frozen and covered with snow).

6 – 8 December 2010 NWFS

- Why 6 – 8 December 2010 case study?
  - Its relatively significant impact on the residents of western North Carolina. Accumulations for the event ranged from about two-to-six inches of snow in the valleys of the Tennessee border counties, to ten inches of snow at the high elevations of the Smoky Mountains, to almost 18 inches of snow in the mountains further to the north of the Smokies in NC.

6 – 8 December 2010 NWFS

One week earlier…

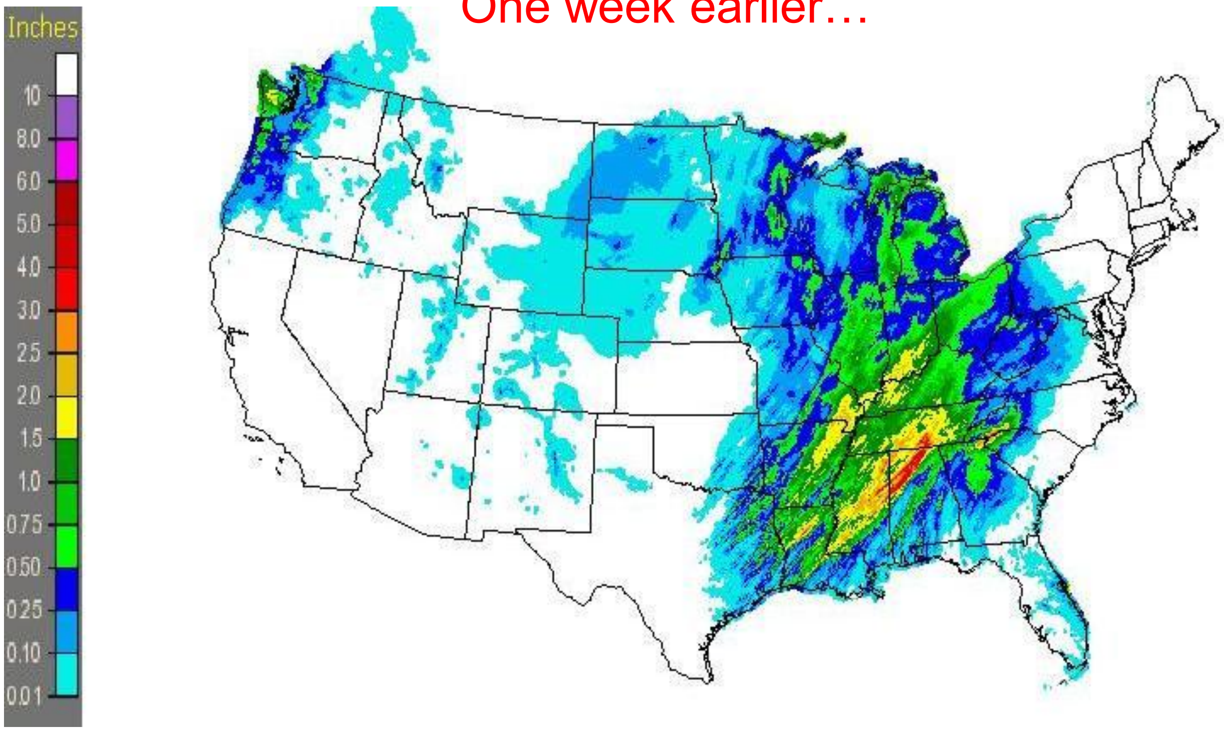

Observed 24-h accumulated precipitation (inches) analysed by the Advanced Hydrologic Prediction Service valid at 1200 UTC 30 November 2010.

6 – 8 December 2010 NWFS

One week earlier…

Observed 24-h accumulated precipitation (inches) analysed by the Advanced Hydrologic Prediction Service valid at 1200 UTC 1 December 2010.

6 – 8 December 2010 NWFS

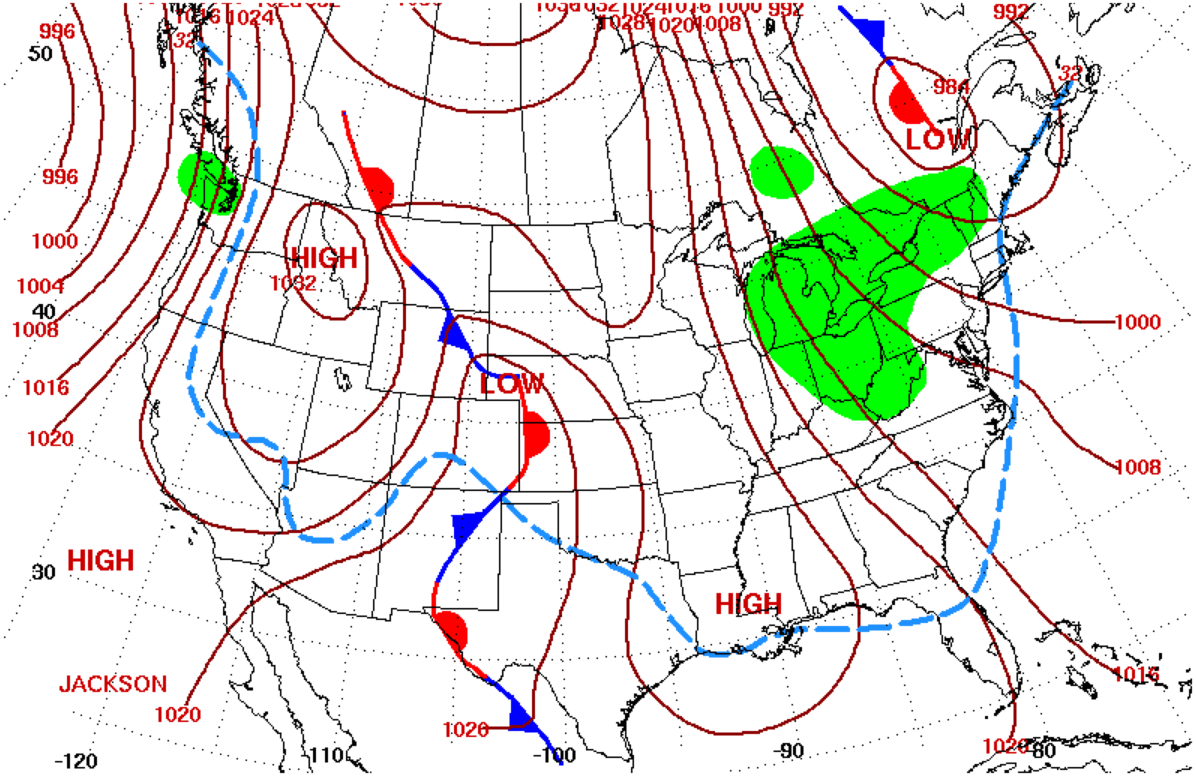

Daily Weather Map of mean sea level pressure (solid contours, interval = 60 m), 0ºC isotherm (dashed), locations of overcast skies (shading), and surface fronts available from the HPC valid 1200 UTC 7 December 2010. {Courtesy: Hydrometeorological Prediction Center.}

6 – 8 December 2010 NWFS

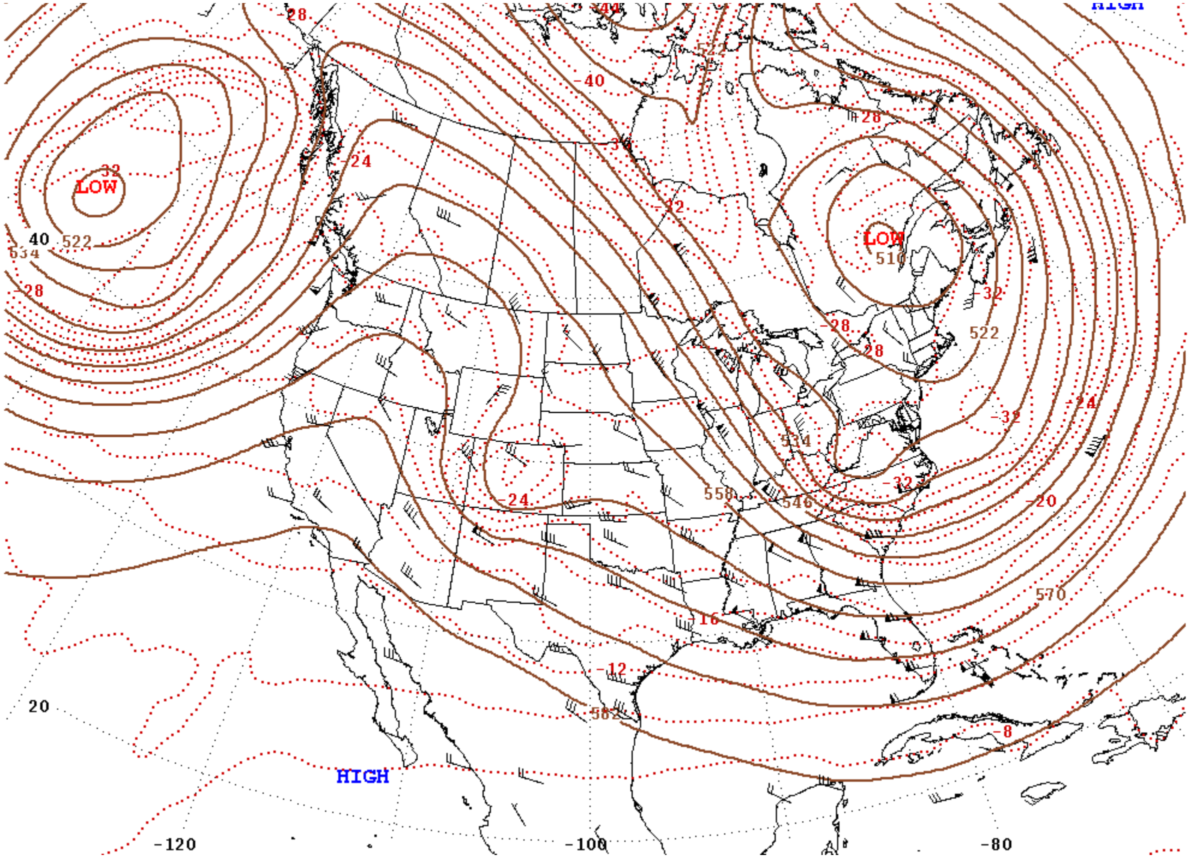

Daily Weather Map of geopotential height (solid contours, interval = 60 m) and temperature (dashed contours, interval = 2°C) at the 500 hPa level available from the HPC valid 1200 UTC 7 December 2010. {Courtesy: Hydrometeorological Prediction Center.}

6 – 8 December 2010 NWFS

- KMRX NEXRAD 0.5^{o} reflectivity loops
  - 1200 UTC 6 – 0000 UTC 7 December 2010
  - 0000 UTC 7 – 0000 UTC 8 December 2010

6 – 8 December 2010 NWFS

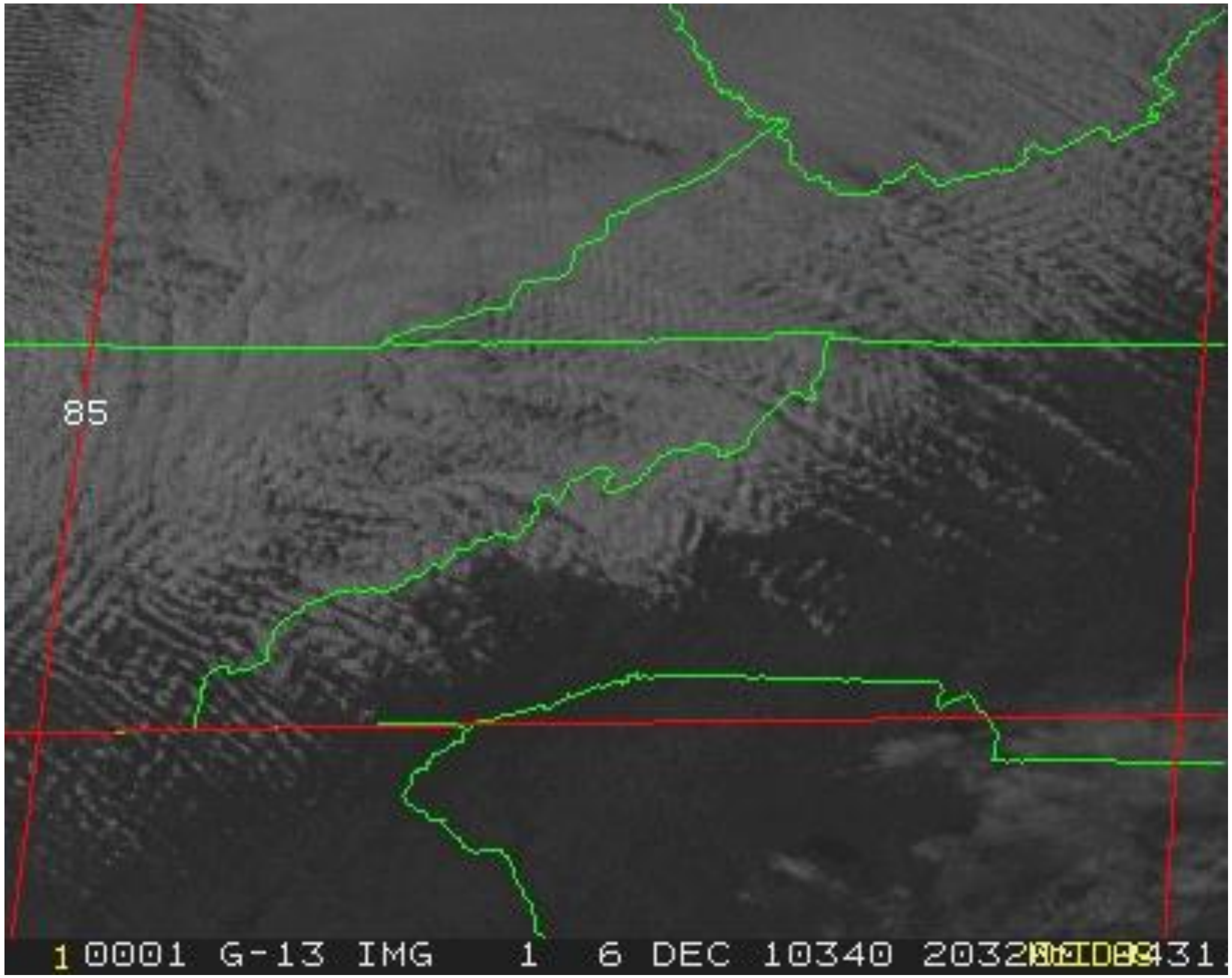

GOES-13 visible imagery valid 2032 UTC 6 December 2010.

6 – 8 December 2010 NWFS

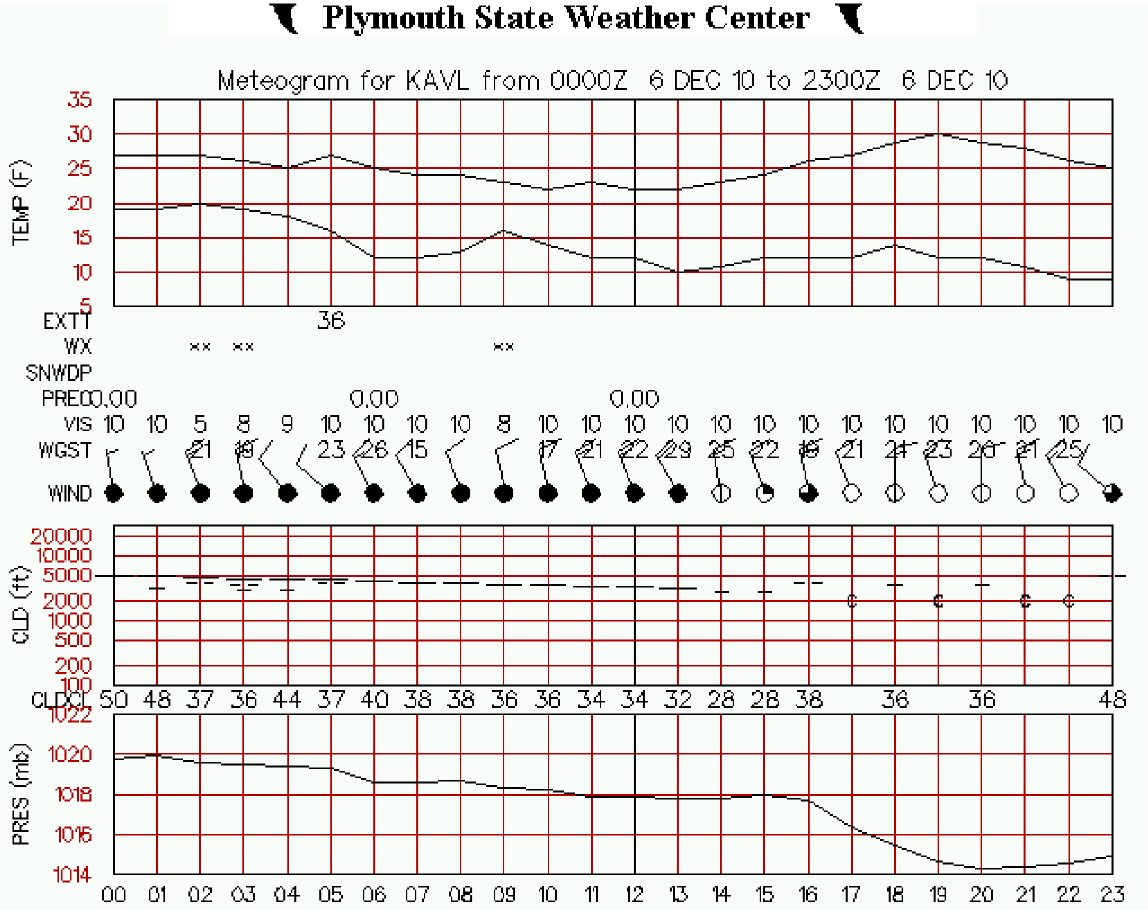

KAVL meteogram valid 6 December 2010.

6 – 8 December 2010 NWFS

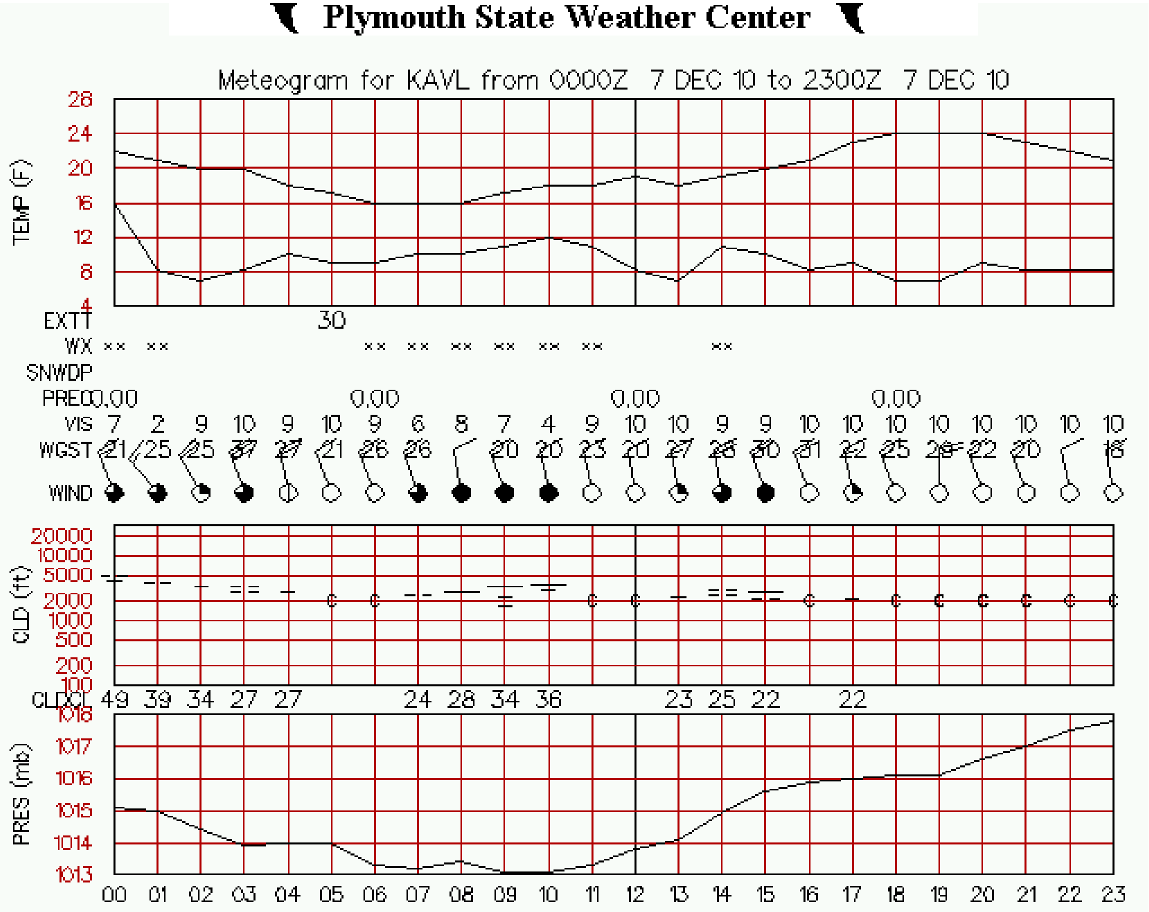

KAVL meteogram valid 7 December 2010.

ARW-WRF simulations

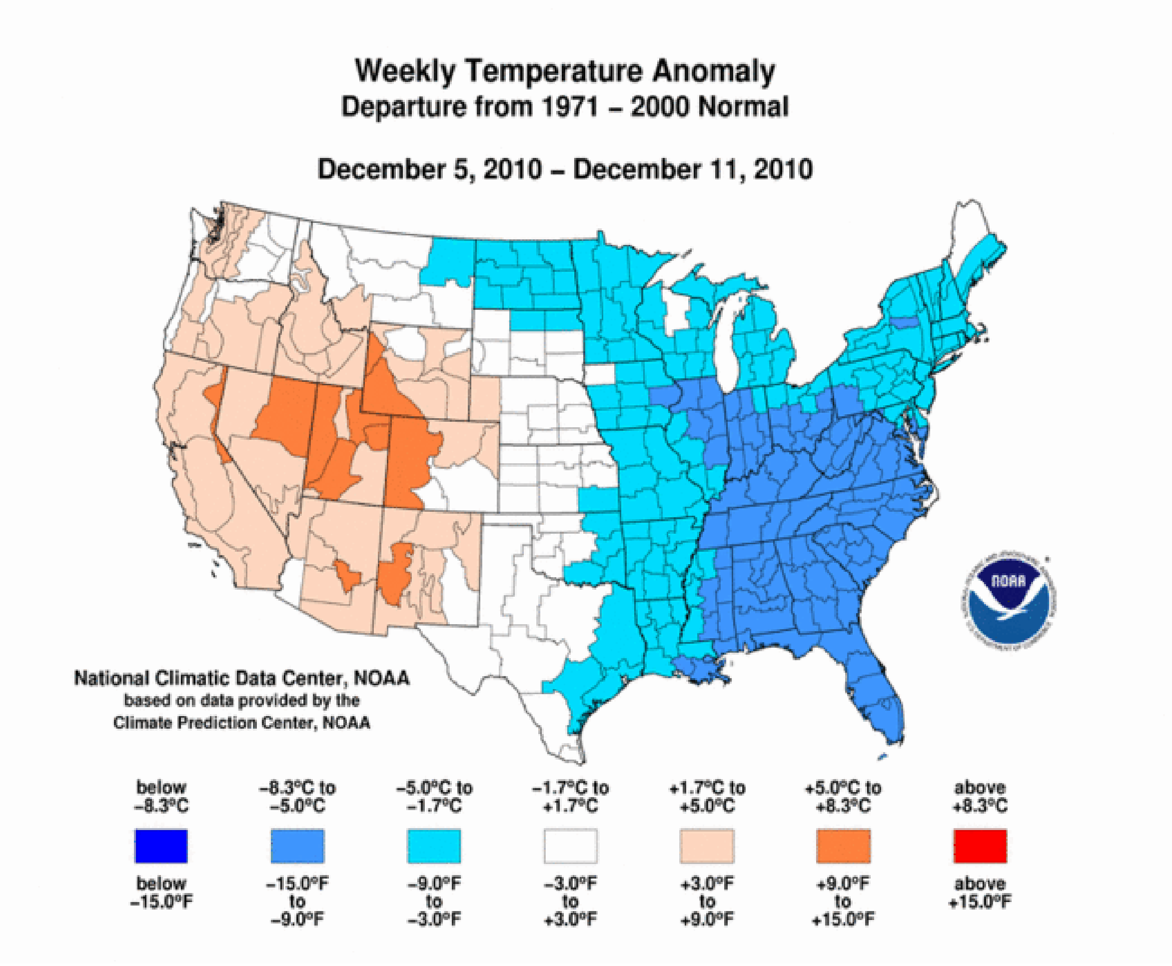

http://www1.ncdc.noaa.gov/pub/data/cmb/images/weekly/us/2010/tanom20101211-pg.gif

WRF Default Simulation

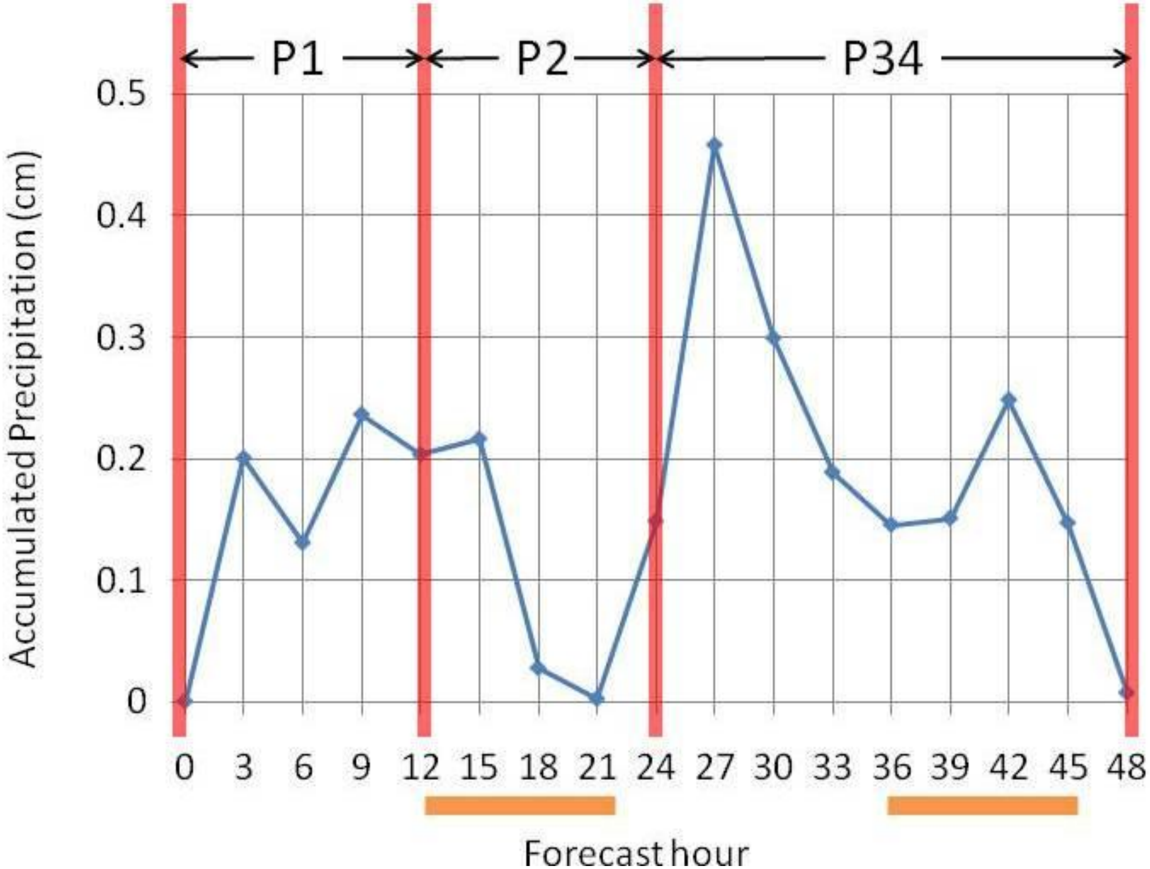

Model simulated 3-h accumulated precipitation (cm) for a location near Max Patch starting at 0000 UTC 6 December 2010. Period designators ‘P1’, ‘P2’, and ‘P34’ are also indicated. Horizontal thick lines indicate the period associated with daylight hours (sunrise; 0725 EST, sunset; 1717 EST).

WRF Default Simulation

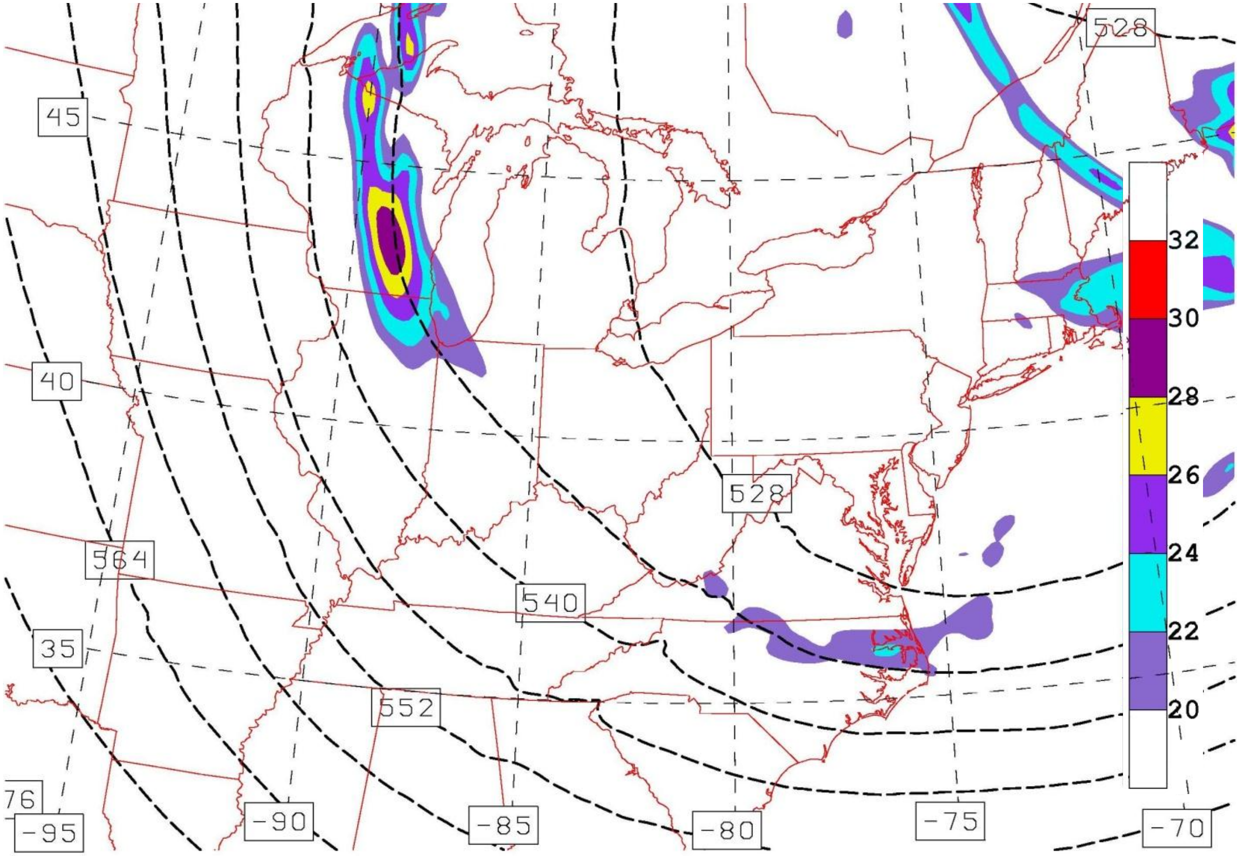

Model simulated 500 hPa level geopotential height (contoured in dashed lines every 6 dm) and absolute vorticity (shading, x 10^{-5} s^{-1}) valid at 1200 UTC 6 December 2010 [F12].

WRF Default Simulation

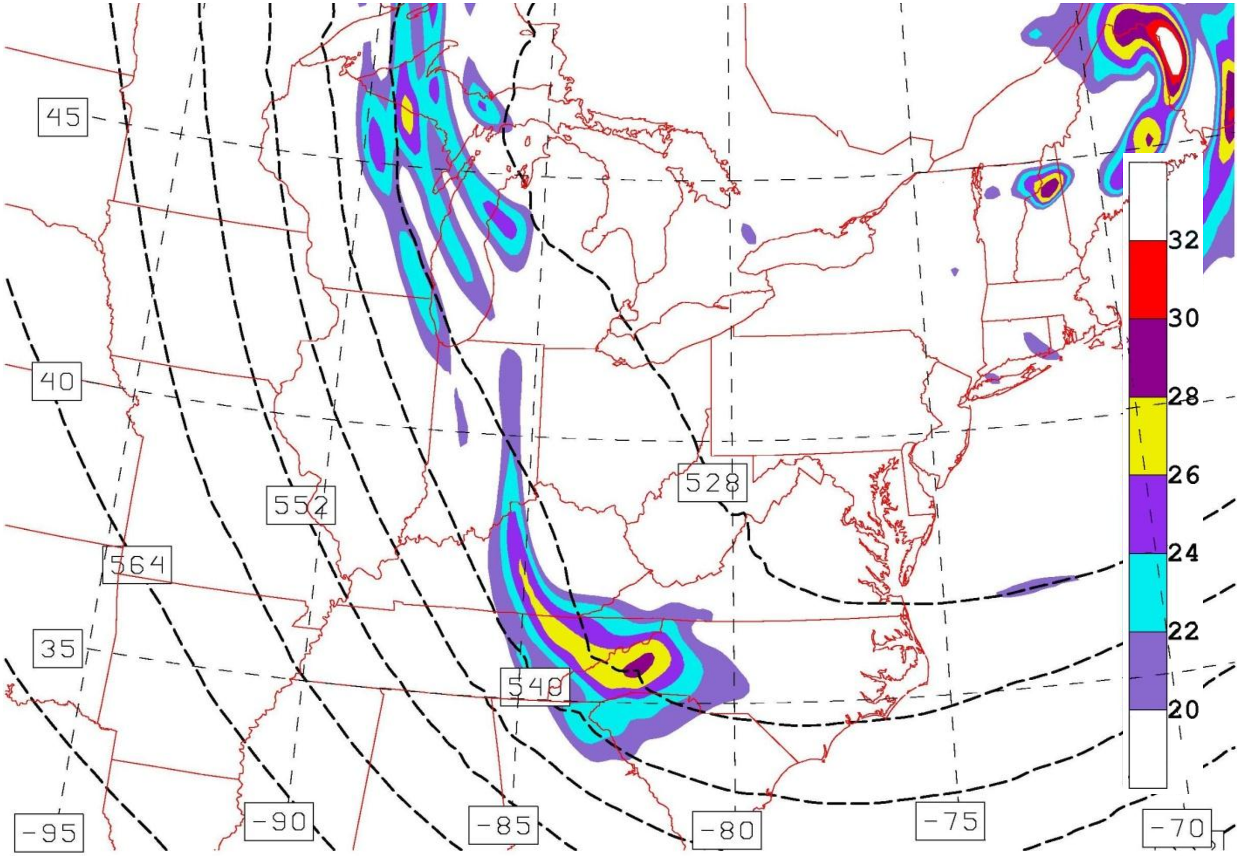

Model simulated 500 hPa level geopotential height (contoured in dashed lines every 6 dm) and absolute vorticity (shading, x 10^{-5} s^{-1}) valid at 0000 UTC 7 December 2010 [F24].

ulation

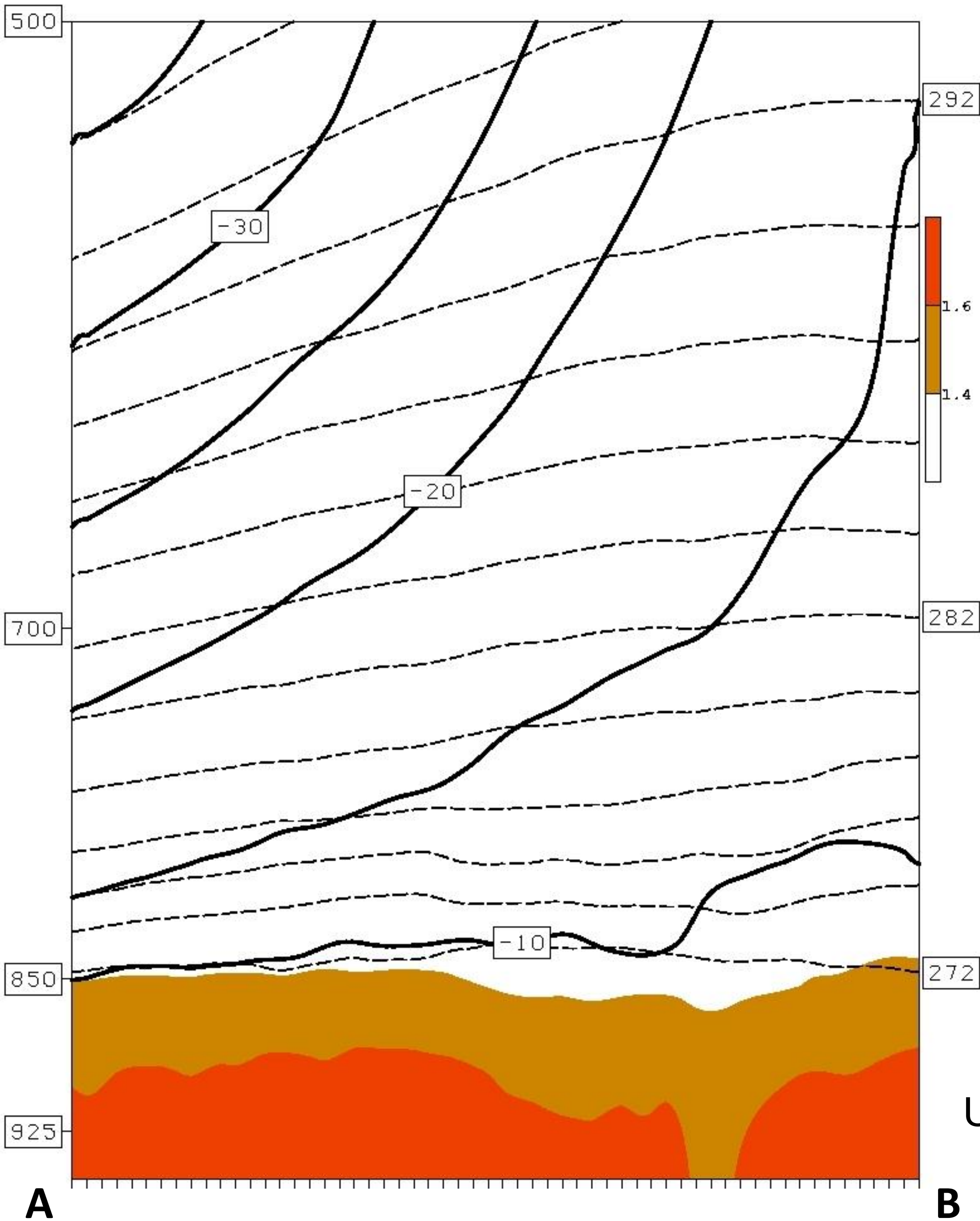

Vertical cross section of model simulated potential temperature (contoured in dashed lines every 2 K), section-normal wind speed (contoured in thick solid lines every 5 m s^{-1}, negative values indicate winds directed out of the page) and vapor mixing ratio (shading for values exceeding 1.4 g kg^{-1}) valid at 2000 UTC 6 December 2010 [F20] located in Kentucky.

Upstream of Cumberland Plateau

WRF Default Simulation

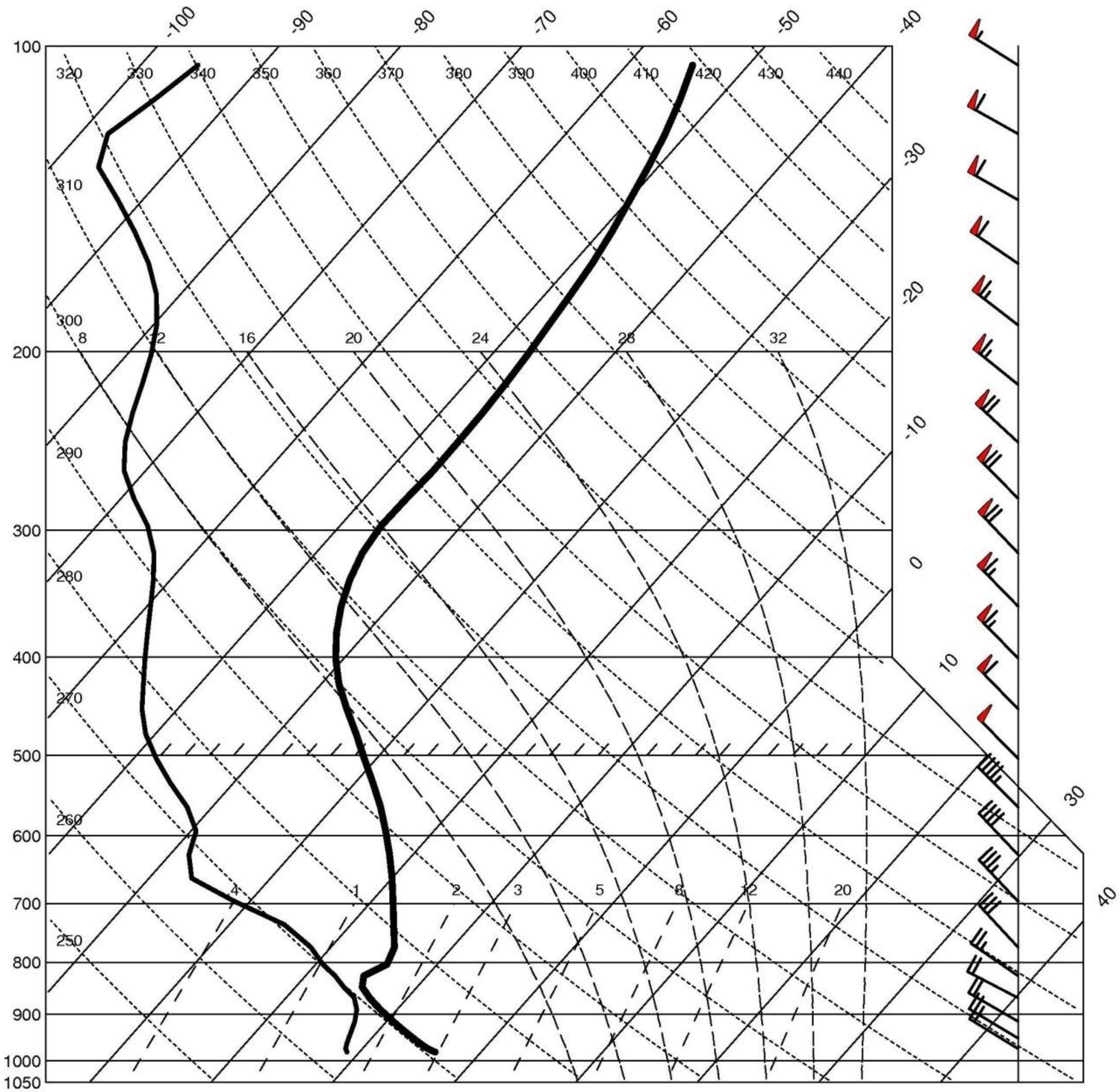

2010120620 Upstream Loc (37.625N, 84.75W) sounding (elv=287 meters)

Model simulated skew-T-log p diagram valid at 2000 UTC 6 December 2010 [F20] at the middle point of the upstream vertical cross section.

WRF Default Simulation

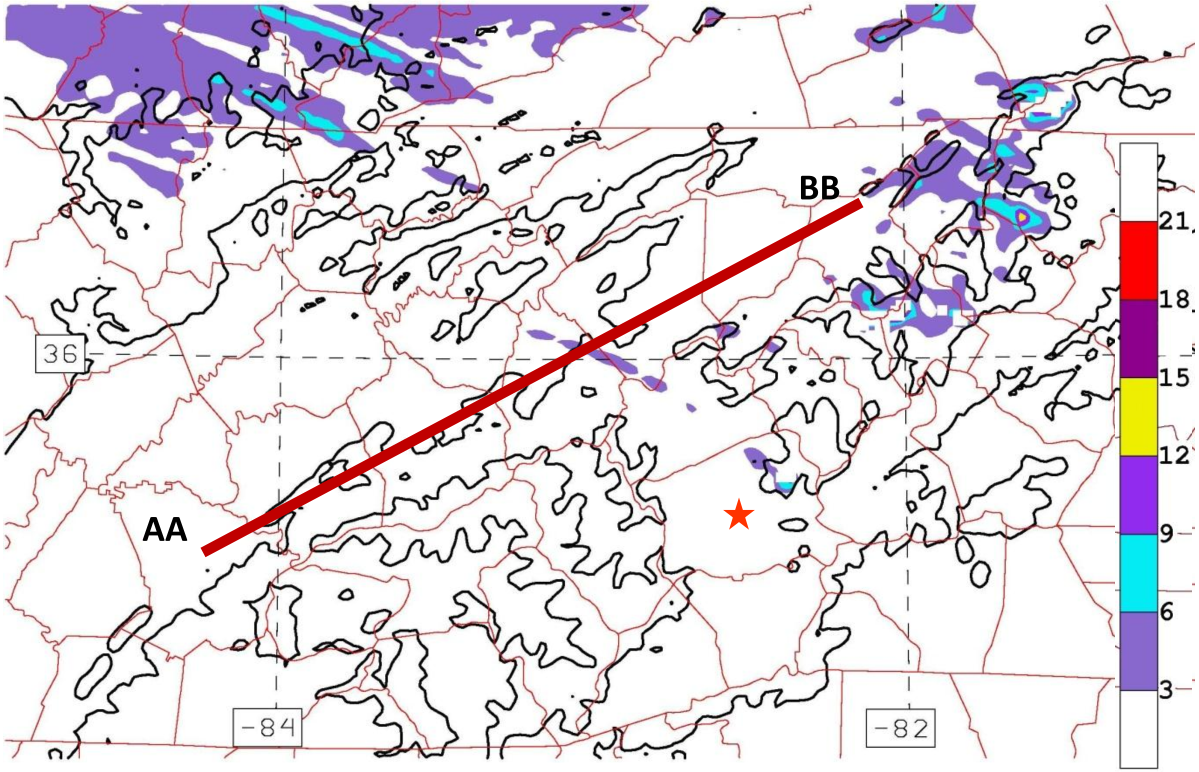

Model simulated 850 hPa level liquid and ice mixing ratio (shading, x 10^{-2} g kg^{-1}) and domain 3 terrain elevation exceeding 0.4 and 1.0 km (contours) valid at 1800 UTC 6 December 2010 [F18]. The star symbol highlights the location of Asheville, NC.

WRF Default Simulation

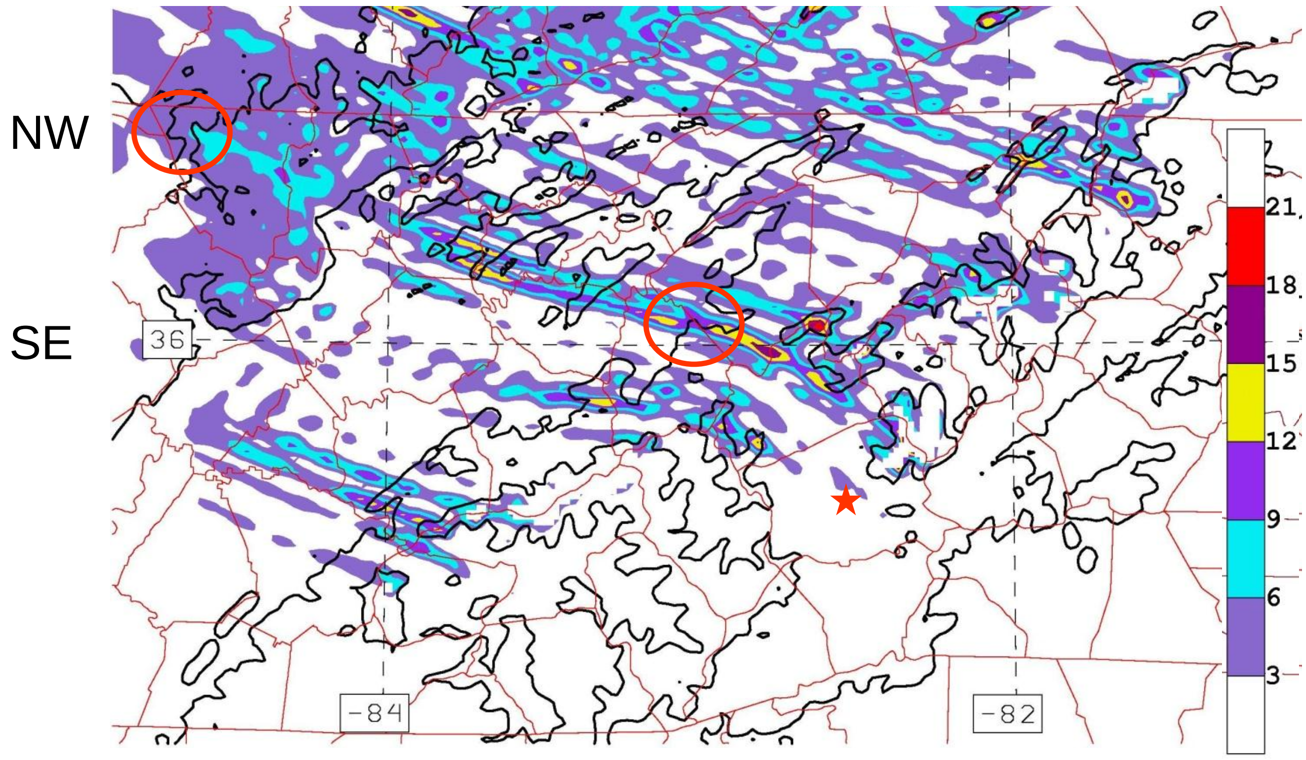

Model simulated 850 hPa level liquid and ice mixing ratio (shading, x 10^{-2} g kg^{-1}) and domain 3 terrain elevation exceeding 0.4 and 1.0 km (contours) valid at 2100 UTC 6 December 2010 [F21]. The star symbol highlights the location of Asheville, NC.

WRF Default Simulation

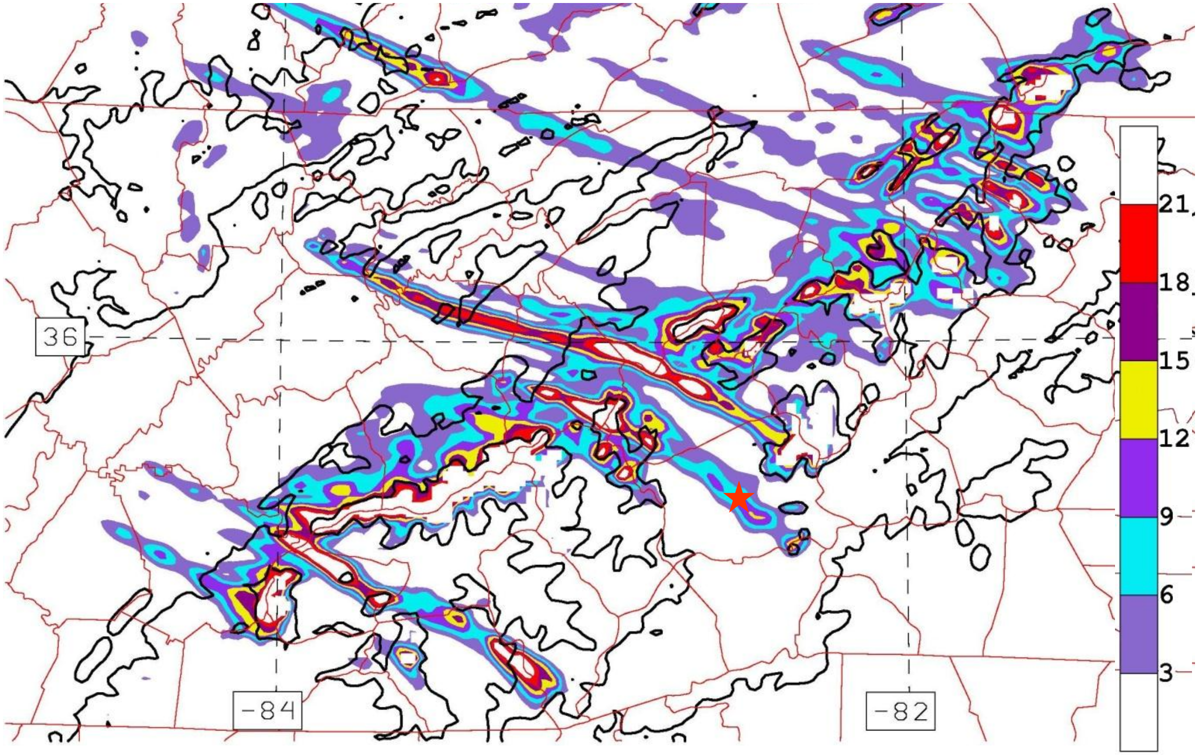

Model simulated 850 hPa level liquid and ice mixing ratio (shading, x 10^{-2} g kg^{-1}) and domain 3 terrain elevation exceeding 0.4 and 1.0 km (contours) valid at 0000 UTC 7 December 2010 [F24]. The star symbol highlights the location of Asheville, NC.

WRF Default Simulation

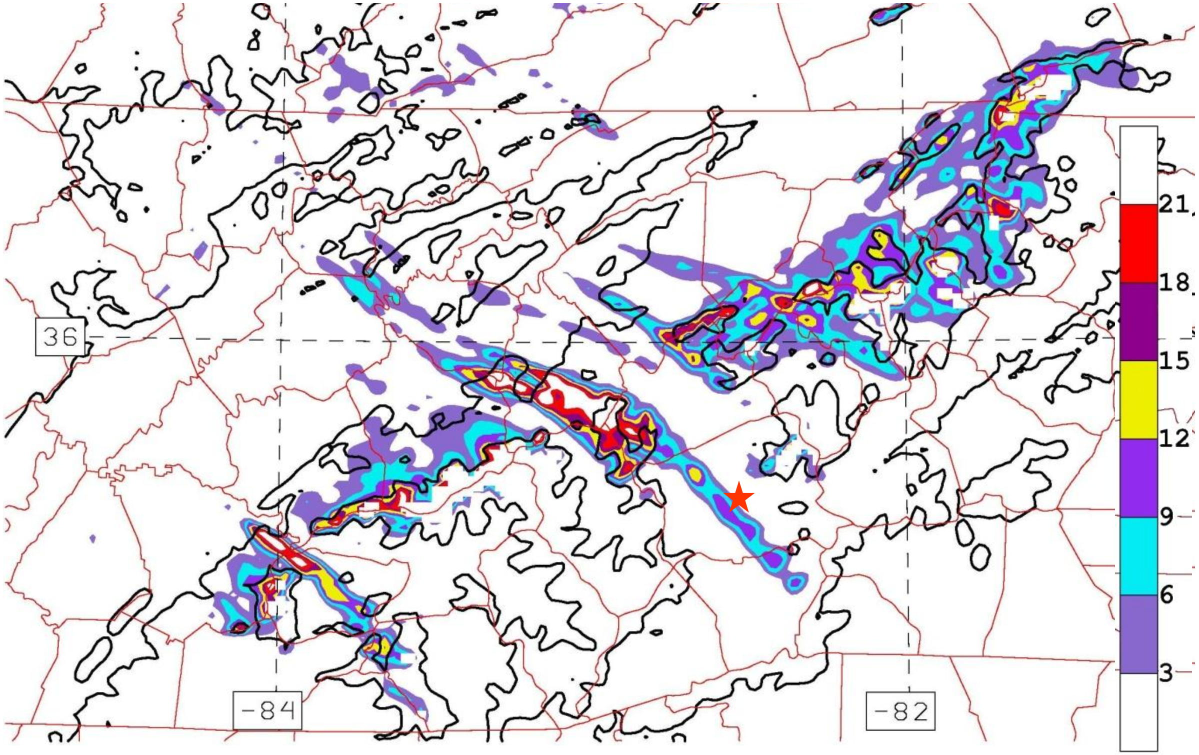

Model simulated 850 hPa level liquid and ice mixing ratio (shading, x 10^{-2} g kg^{-1}) and domain 3 terrain elevation exceeding 0.4 and 1.0 km (contours) valid at 0300 UTC 7 December 2010 [F27]. The star symbol highlights the location of Asheville, NC.

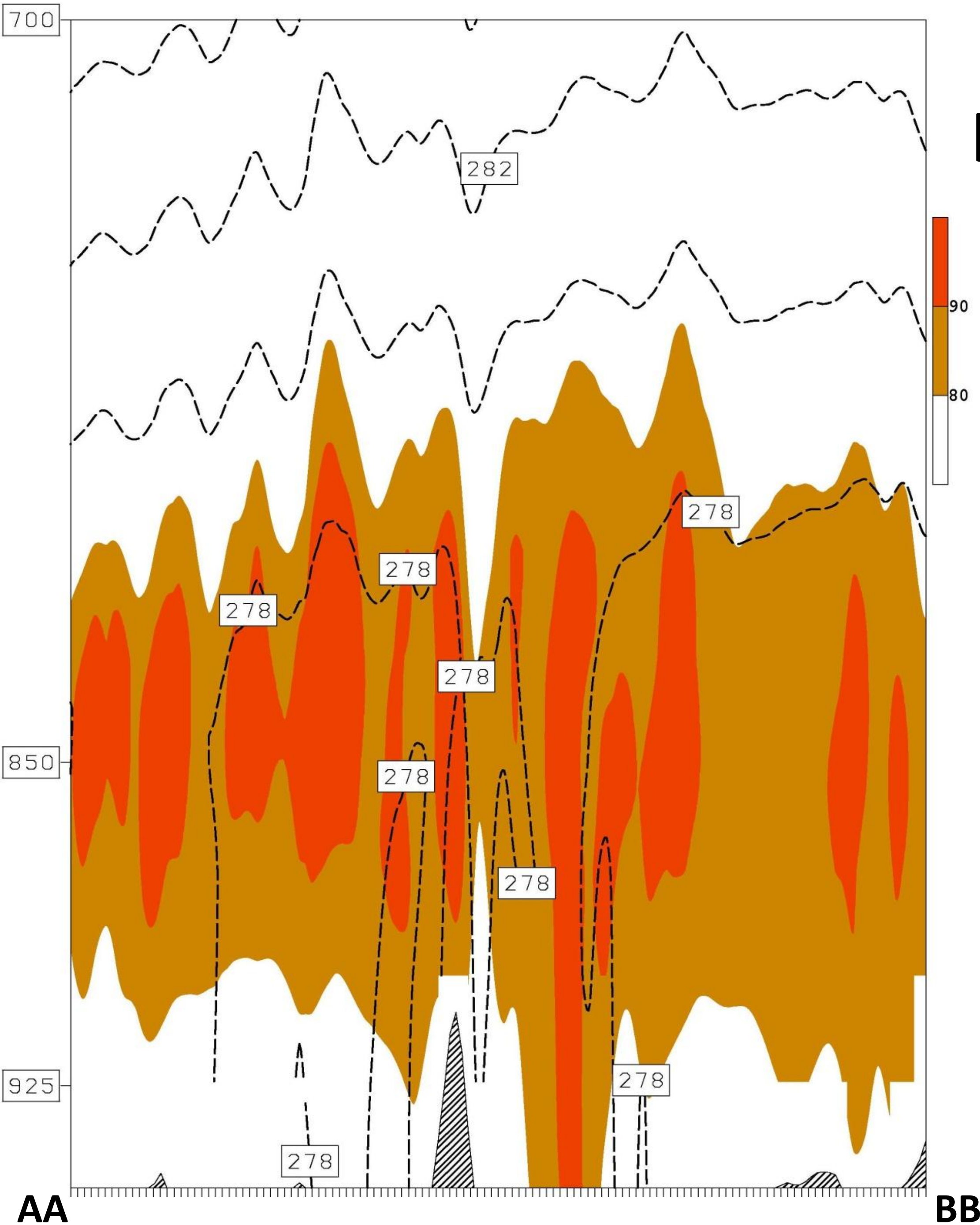

mulation

Vertical cross section of model simulated equivalent potential temperature (contoured in dashed lines every 2 K) and relative humidity (shading for values exceeding 80%) valid at 0000 UTC 7 December 2010 [F24].

Upstream of NC/TN border

WRF Default Simulation

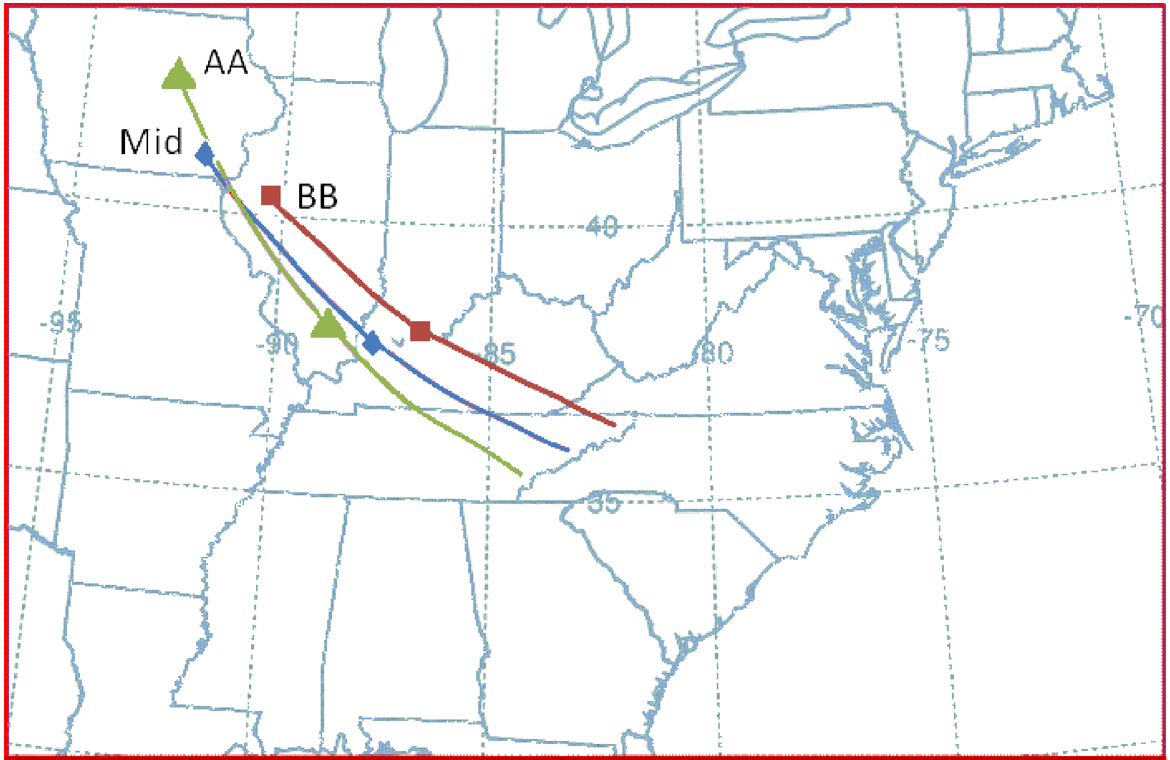

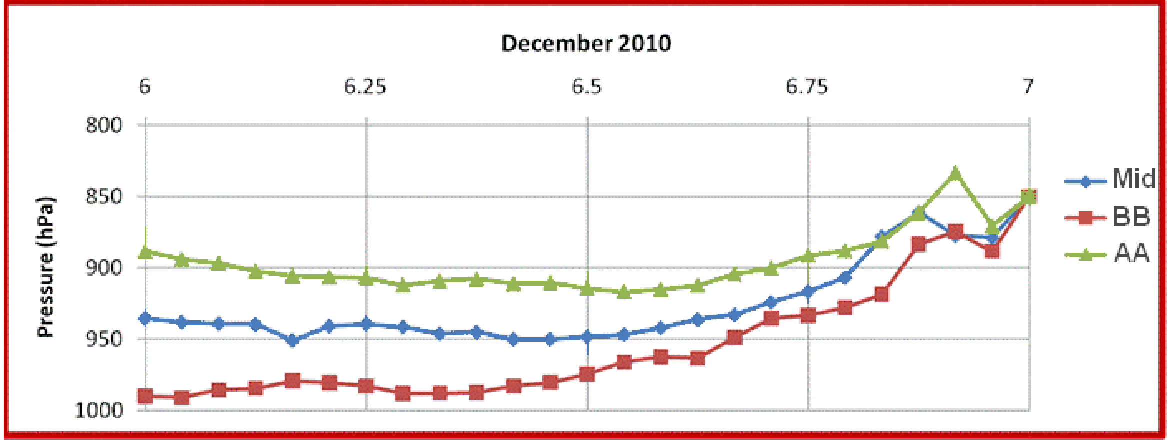

Model simulated 24-h trajectories (0000 UTC 6 – 7 December 2010) analysed by HYSPLIT for air parcels ending at the end points (AA=▲, BB=■) and middle point (Mid=♦) of the vertical cross section shown in the previous figure at the 850 hPa level (middle of the cloud layer).

mulation

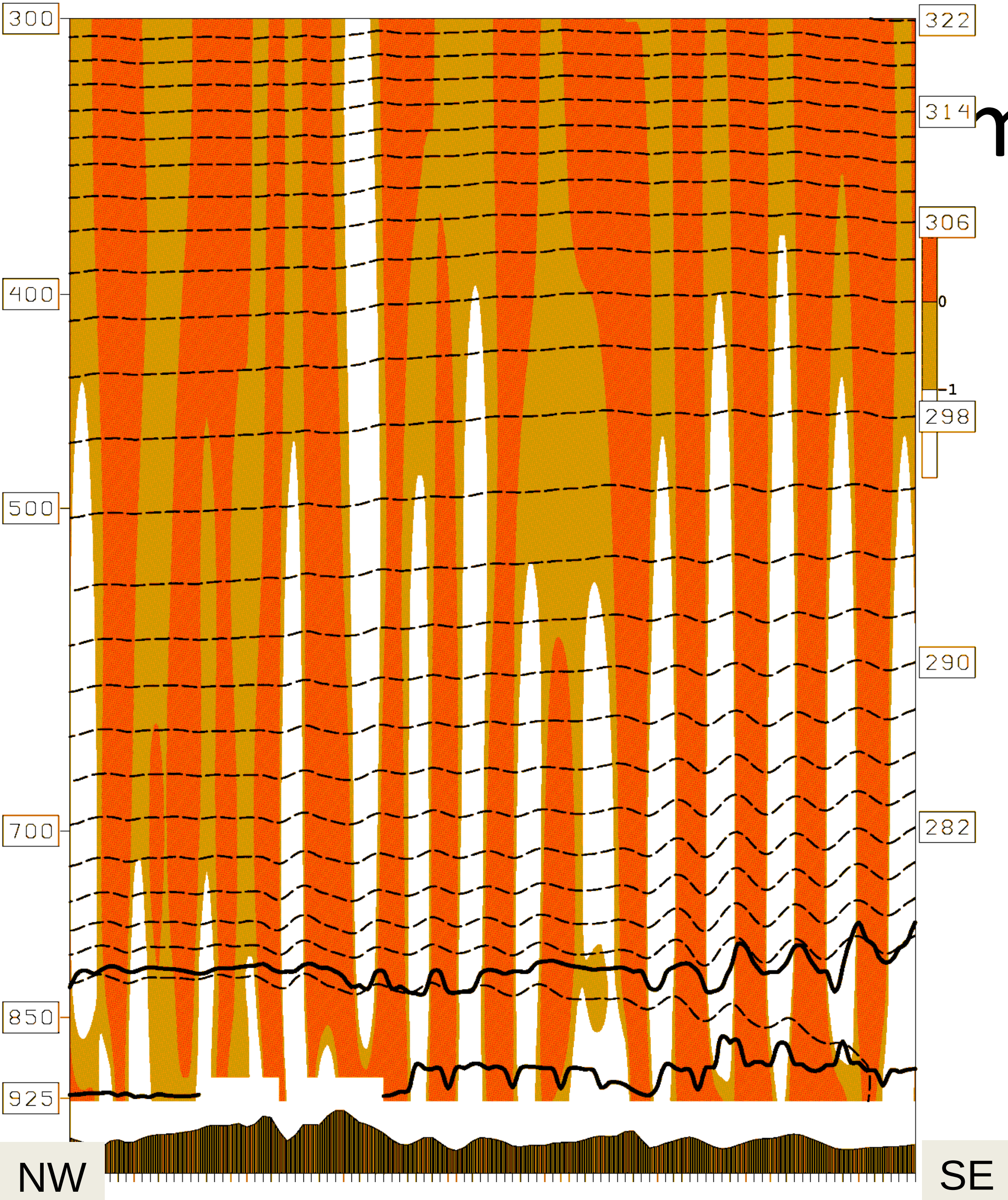

Model simulated vertical motion (shading, hPa s^{-1}), cloud mixing ratio (thick solid contour 1×10^{-2} g kg^{-1}), and potential temperature (contoured in dashed lines every 2 K) valid at 2100 UTC 6 December 2010 [F21] in a vertical cross section oriented along the cloud band labeled NW-SE in a previous figure. The horizontal distance between vertical motion crests is approximately 10 km.

Band-parallel section

WRF Default Simulation

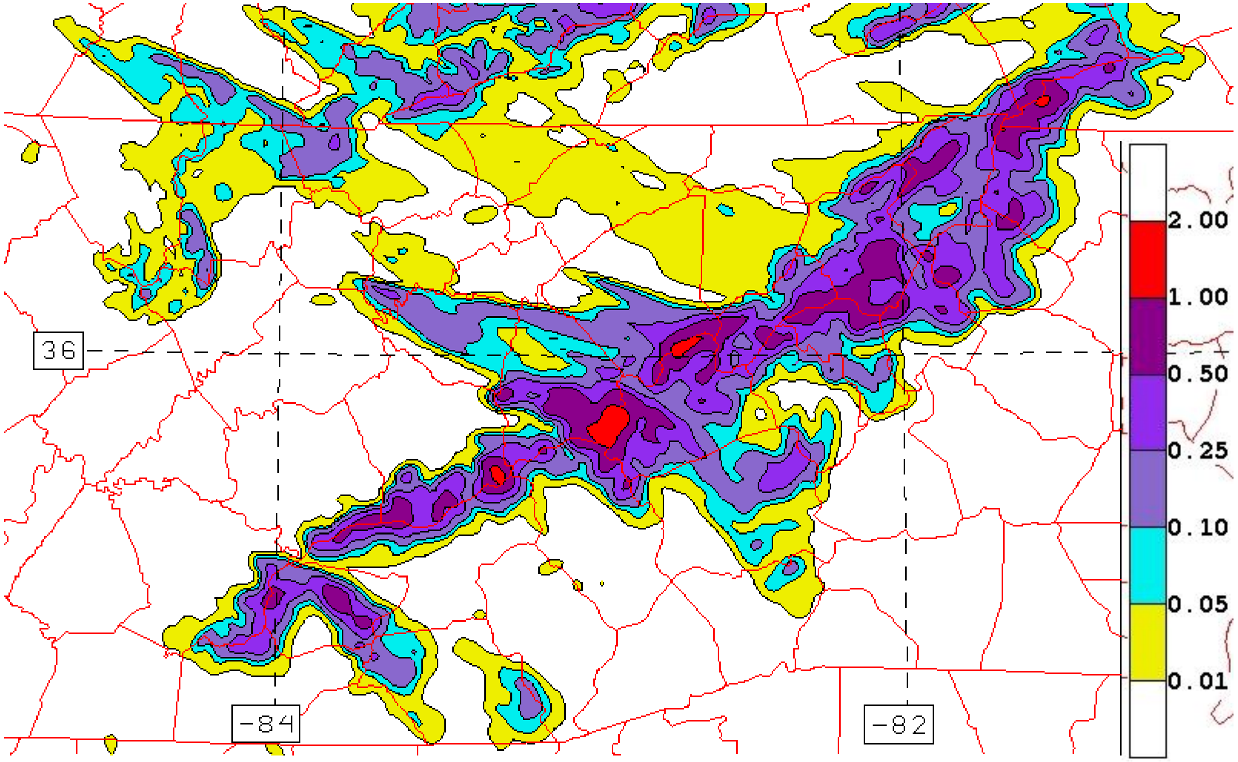

Model simulated 24-h liquid equivalent accumulated precipitation (cm) for the period ending 0000 UTC 8 December 2010 [period designated 'P34'] for the experiment having the default SH flux parameterization scheme "on" during the entire model simulation.

WRF SHF experiments

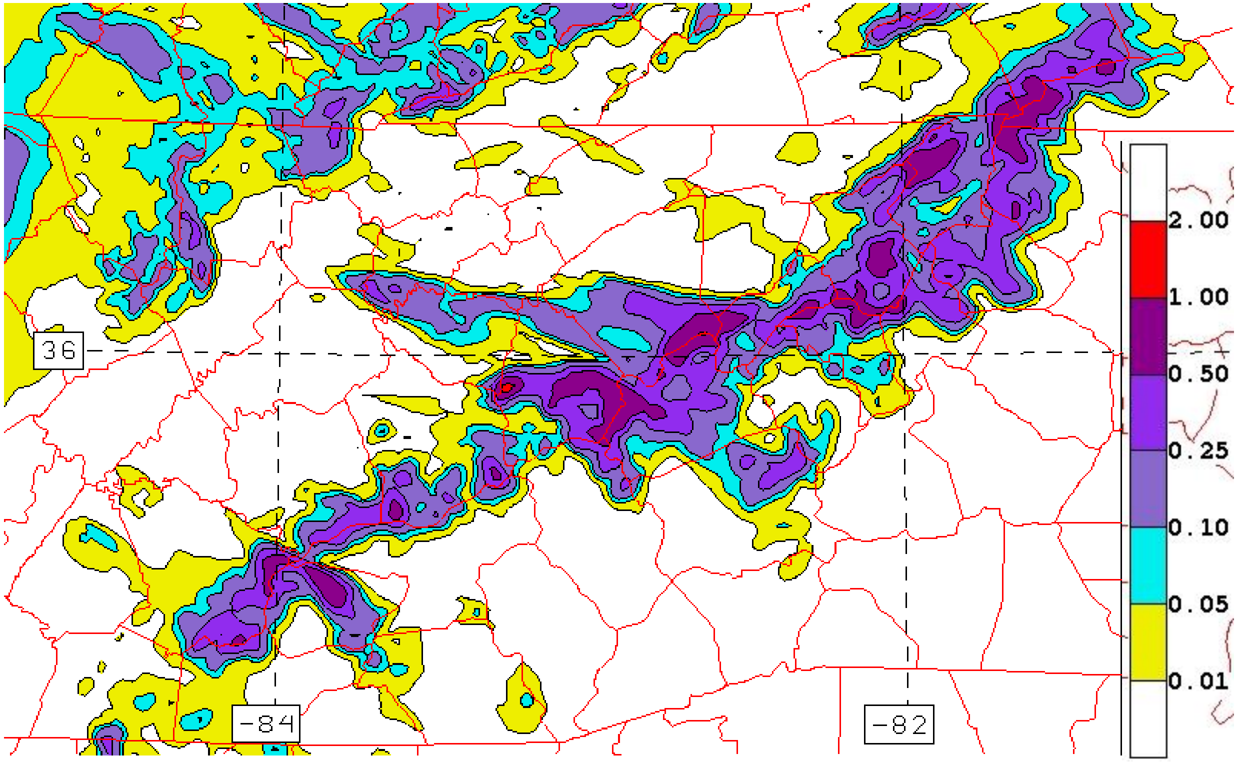

Model simulated 24-h liquid equivalent accumulated precipitation (cm) for the period ending 0000 UTC 8 December 2010 [period designated ‘P34’] for the experiment having the default SH flux parameterization scheme <u>“off” during P2</u>.

WRF SHF experiments

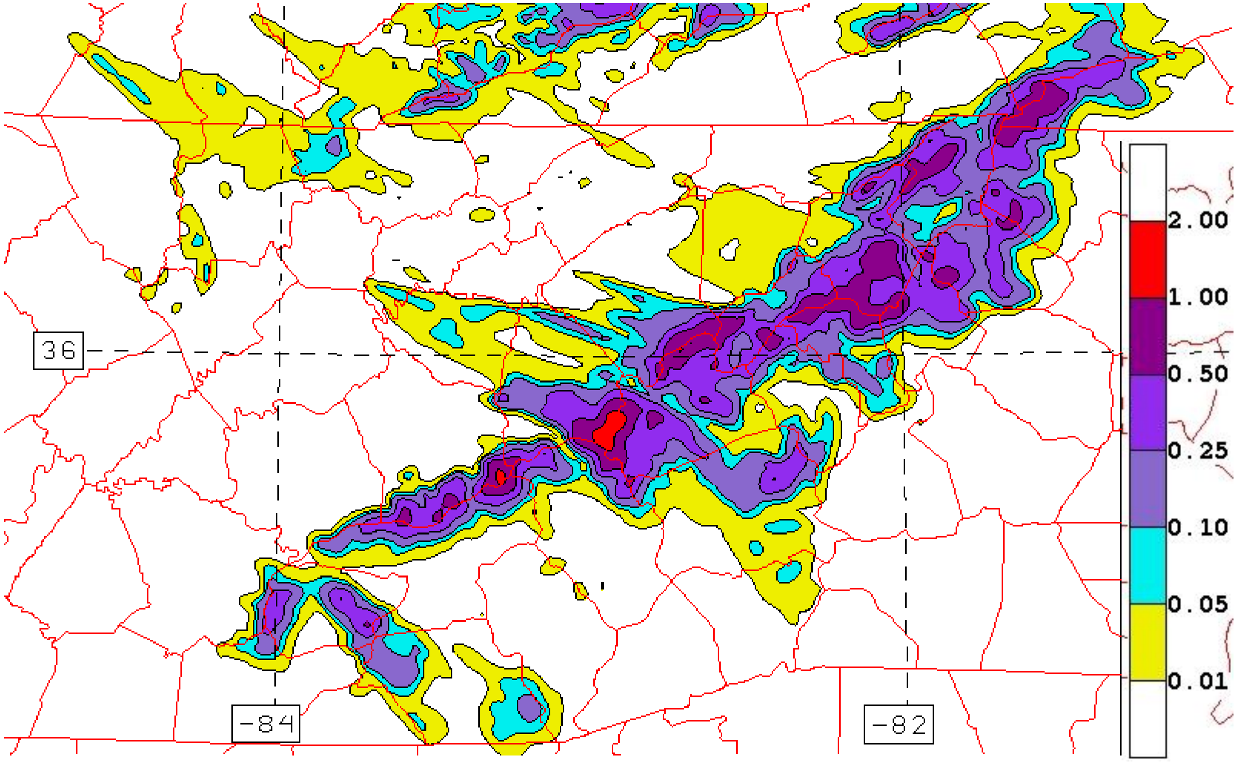

Model simulated 24-h liquid equivalent accumulated precipitation (cm) for the period ending 0000 UTC 8 December 2010 [period designated 'P34'] for the experiment having the enhanced SH flux parameterization scheme "on" during the entire model simulation.

WRF SHF experiments

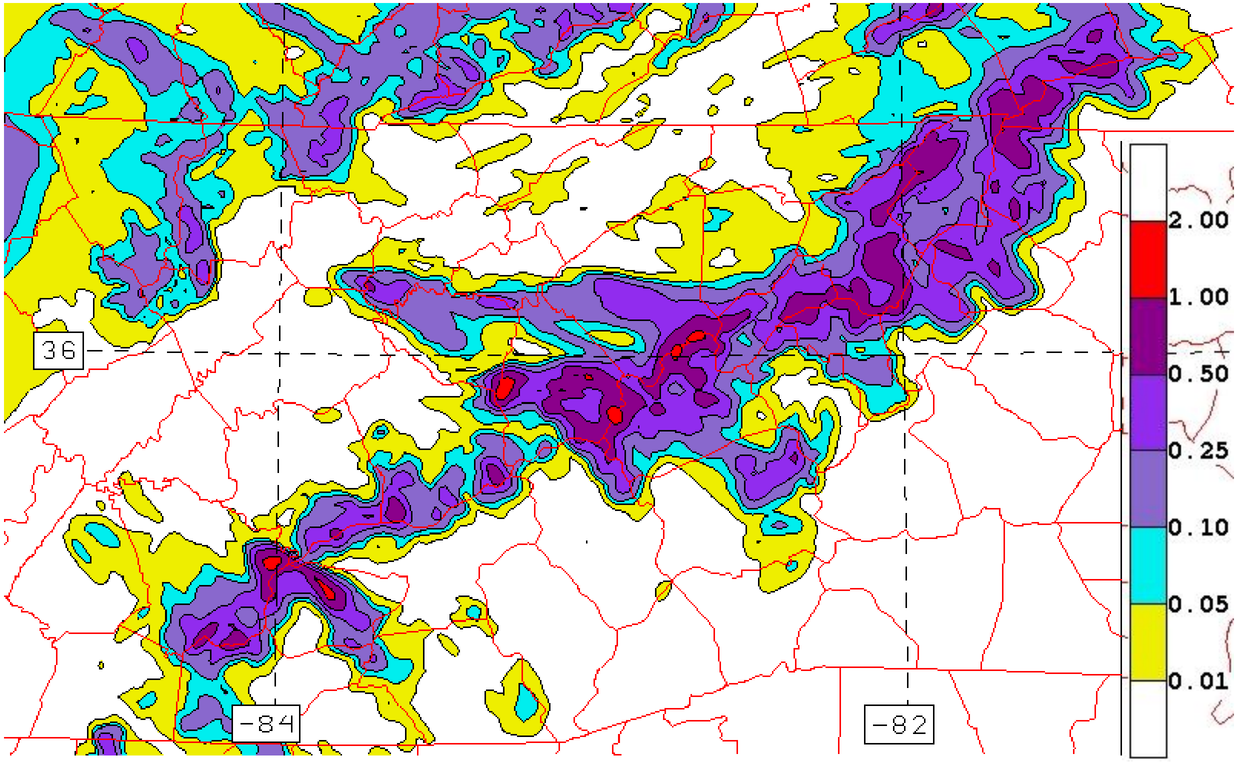

Model simulated 24-h liquid equivalent accumulated precipitation (cm) for the period ending 0000 UTC 8 December 2010 [period designated 'P34'] for the experiment having the SH fluxes shut "off" during the entire model simulation.

WRF SHF experiments

Model simulated 24-h liquid equivalent accumulated precipitation (cm) statistics

Surface SH flux parameterization	**SH scheme "off"**	**Exp. mean (cm)**	**"on" mean (cm)**	**Exp. σ (cm)**	**"on" σ (cm)**	**RMSE (cm)**	**Bias (cm)**	**N**
default	P1	0.188	0.182	0.208	0.202	0.027	+0.006	10949
default	P2	0.134	0.147	0.156	0.195	0.113	-0.013	13635
default	P34	0.201	0.173	0.228	0.201	0.060	+0.028	11531
50% enhancement	P1	0.148	0.144	0.190	0.184	0.025	+0.004	10716
50% enhancement	P2	0.125	0.116	0.146	0.175	0.125	+0.009	13331
50% enhancement	P34	0.167	0.139	0.222	0.182	0.064	+0.028	11174
N/A	ALL	0.162	0.128/ 0.098	0.181	0.187/ 0.166	0.122/ 0.146	+0.035/ +0.064	15767

Only default and experiment grid points having at least one simulation whose 24-h liquid equivalent accumulated precipitation amount exceeding 0.025 cm are included in the statistics.

riments

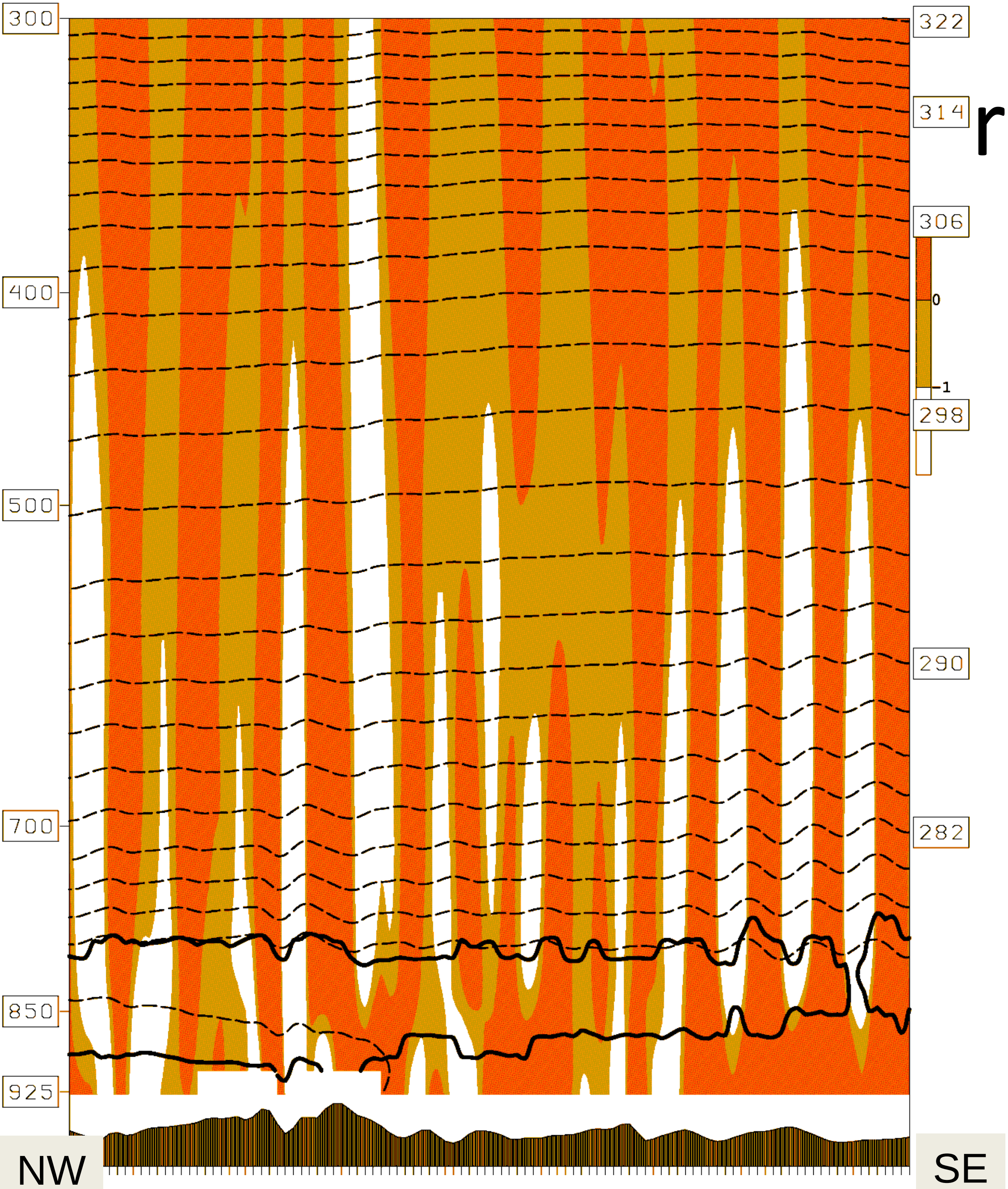

Model simulated vertical motion (shading, hPa s^{-1}), cloud mixing ratio (thick solid contour 1 x 10^{-2} g kg^{-1}), and potential temperature (contoured in dashed lines every 2 K) valid at 2100 UTC 6 December 2010 [F21] for the <u>enhanced SH flux parameterization scheme</u> "on" during the entire model simulation.

Band-parallel section

riments

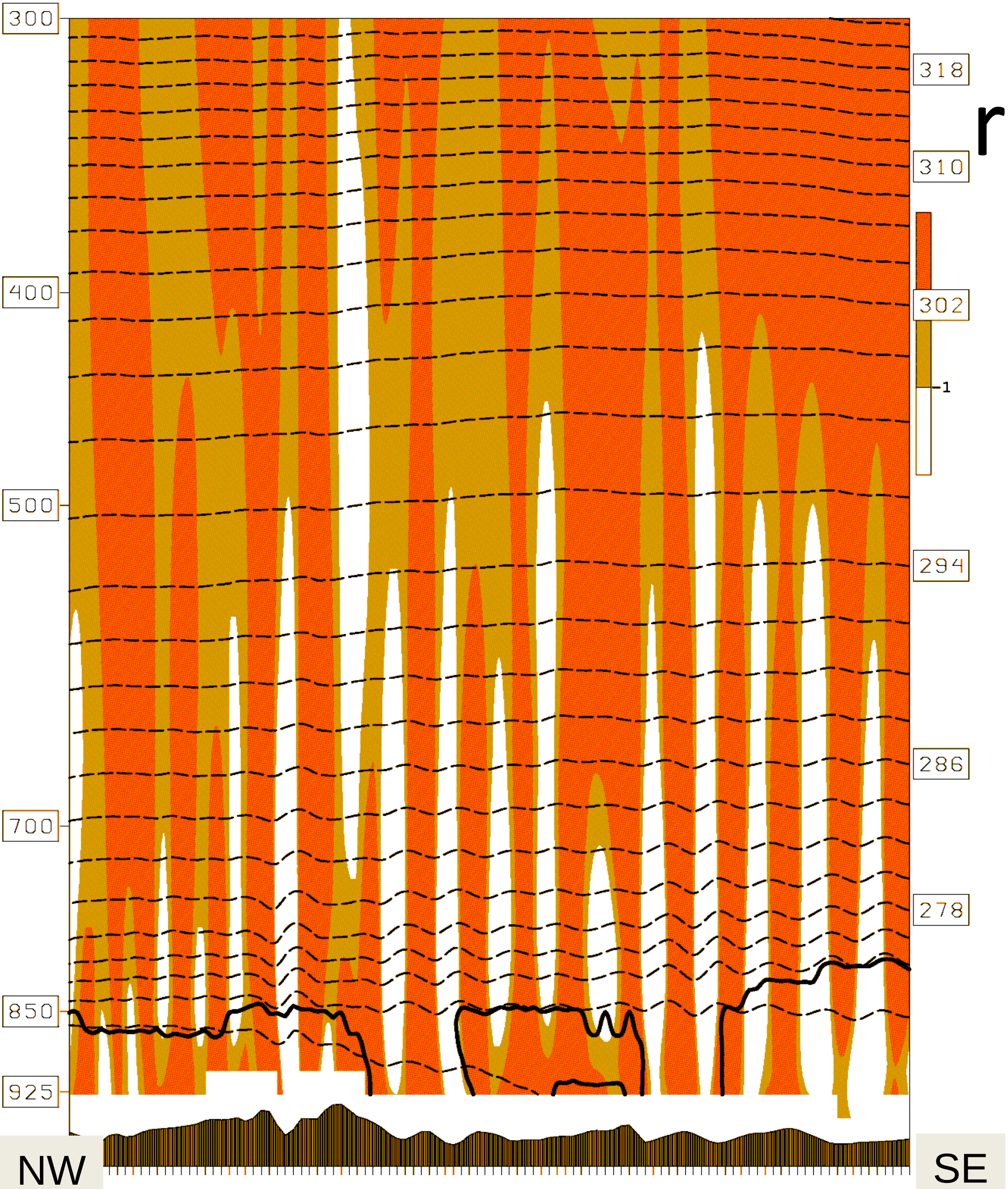

Model simulated vertical motion (shading, hPa s^{-1}), cloud mixing ratio (thick solid contour 1 x 10^{-2} g kg^{-1}), and potential temperature (contoured in dashed lines every 2 K) valid at 2100 UTC 6 December 2010 [F21] for the SH fluxes shut "off" during the entire model simulation.

Band-parallel section

D20

WRF SHF experiments

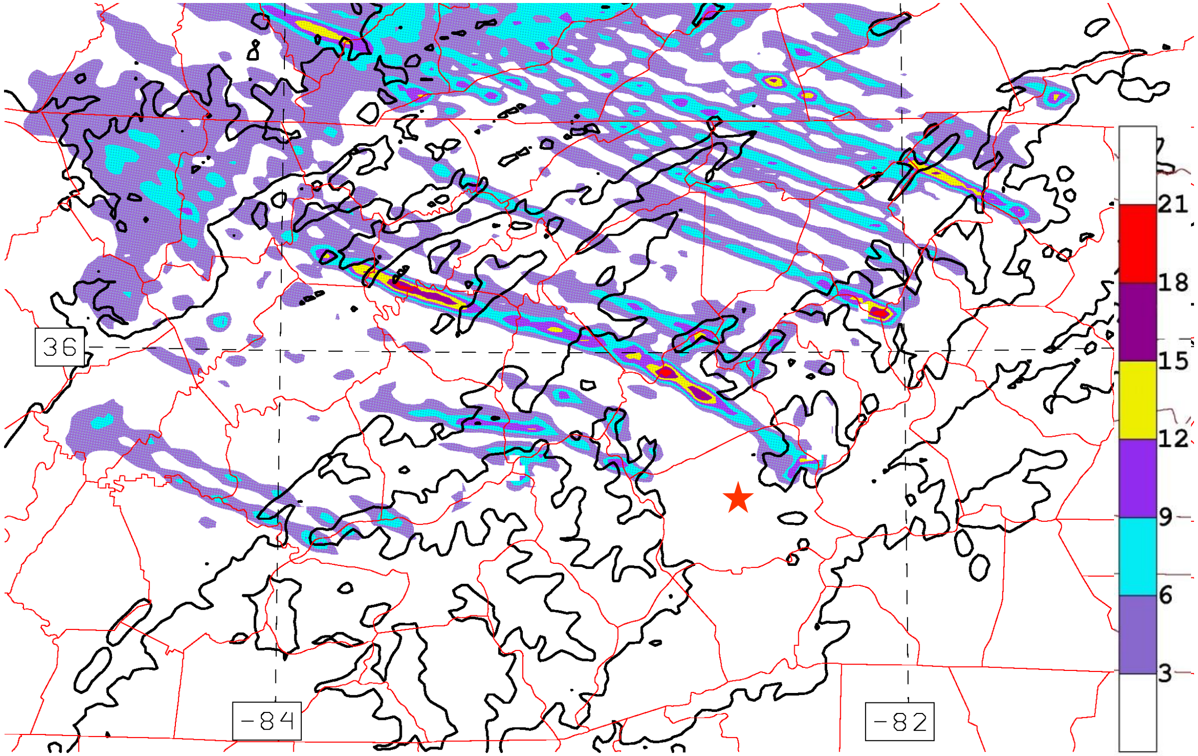

Model simulated liquid and ice mixing ratio (shading, x 10^{-2} g kg^{-1}) and domain 3 terrain elevation exceeding 0.4 and 1.0 km (contours) valid at 2100 UTC 6 December [F21] at the 825 hPa level for the enhanced surface SH flux experiment.

WRF SHF experiments

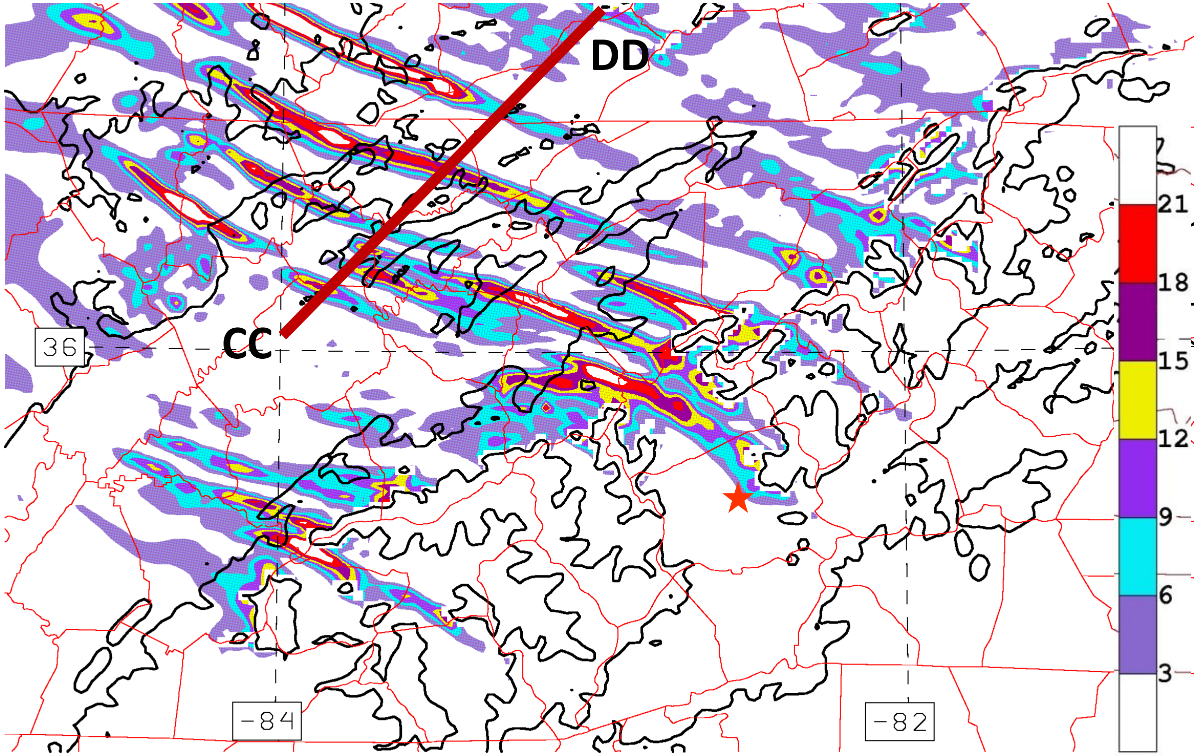

Model simulated liquid and ice mixing ratio (shading, x 10^{-2} g kg^{-1}) and domain 3 terrain elevation exceeding 0.4 and 1.0 km (contours) valid at 2100 UTC 6 December [F21] at the 900 hPa level for the zero surface SH flux experiment. Line marked CC-DD is the orientation of the vertical cross section shown in an upcoming vertical cross section.

eriments

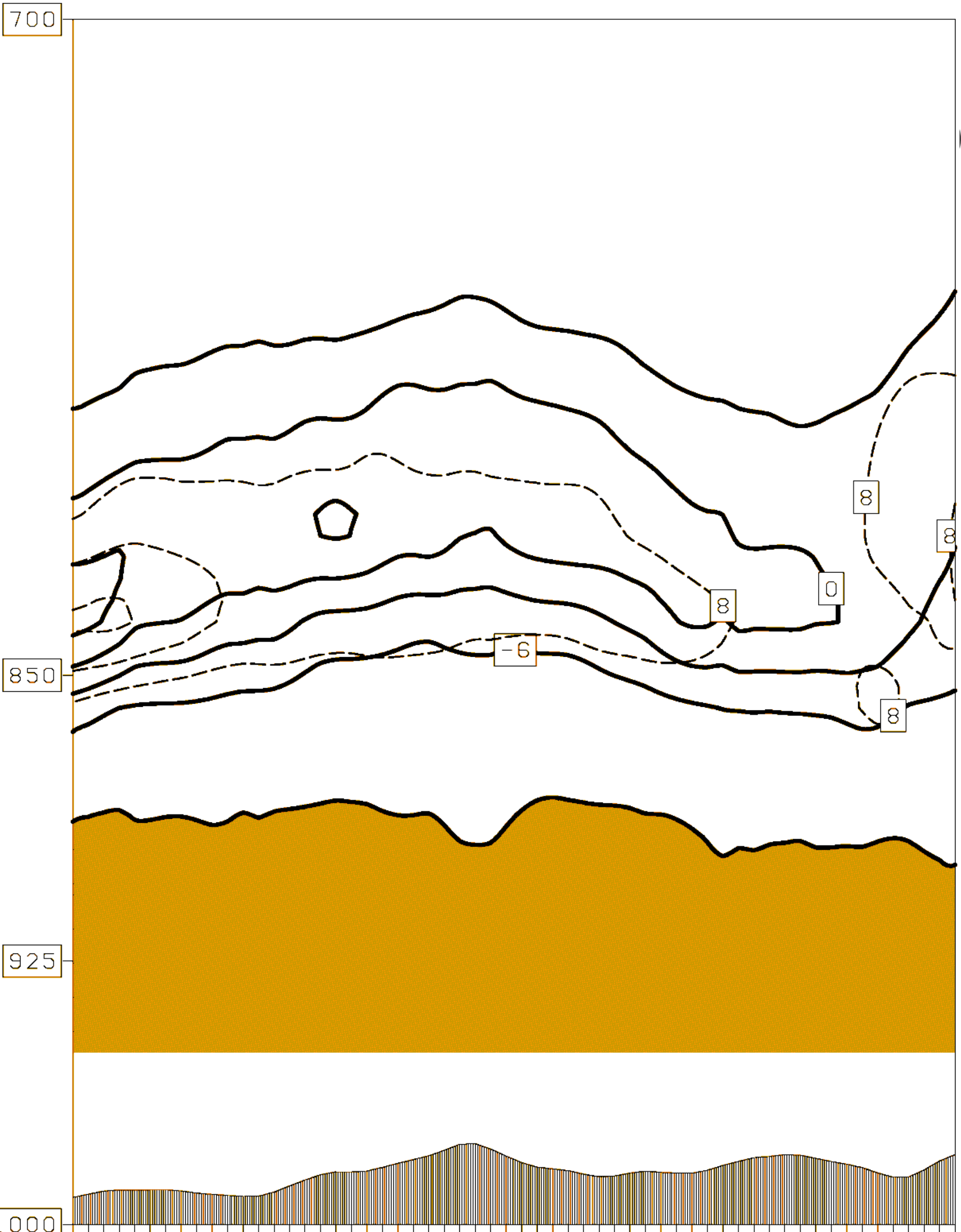

A

B

Model simulated environmental lapse rate (contoured in solid lines every 3°C km^{-1}) and wind shear (contoured in dashed lines; 8 and 12 x 10^{-3} s^{-1}) with steep lapse rates (magnitude exceeding 9°C km^{-1}) shaded valid at 1800 UTC 6 December [F18] for the enhanced surface SH flux experiment. Section is located in Kentucky.

Upstream of Cumberland Plateau

eriments

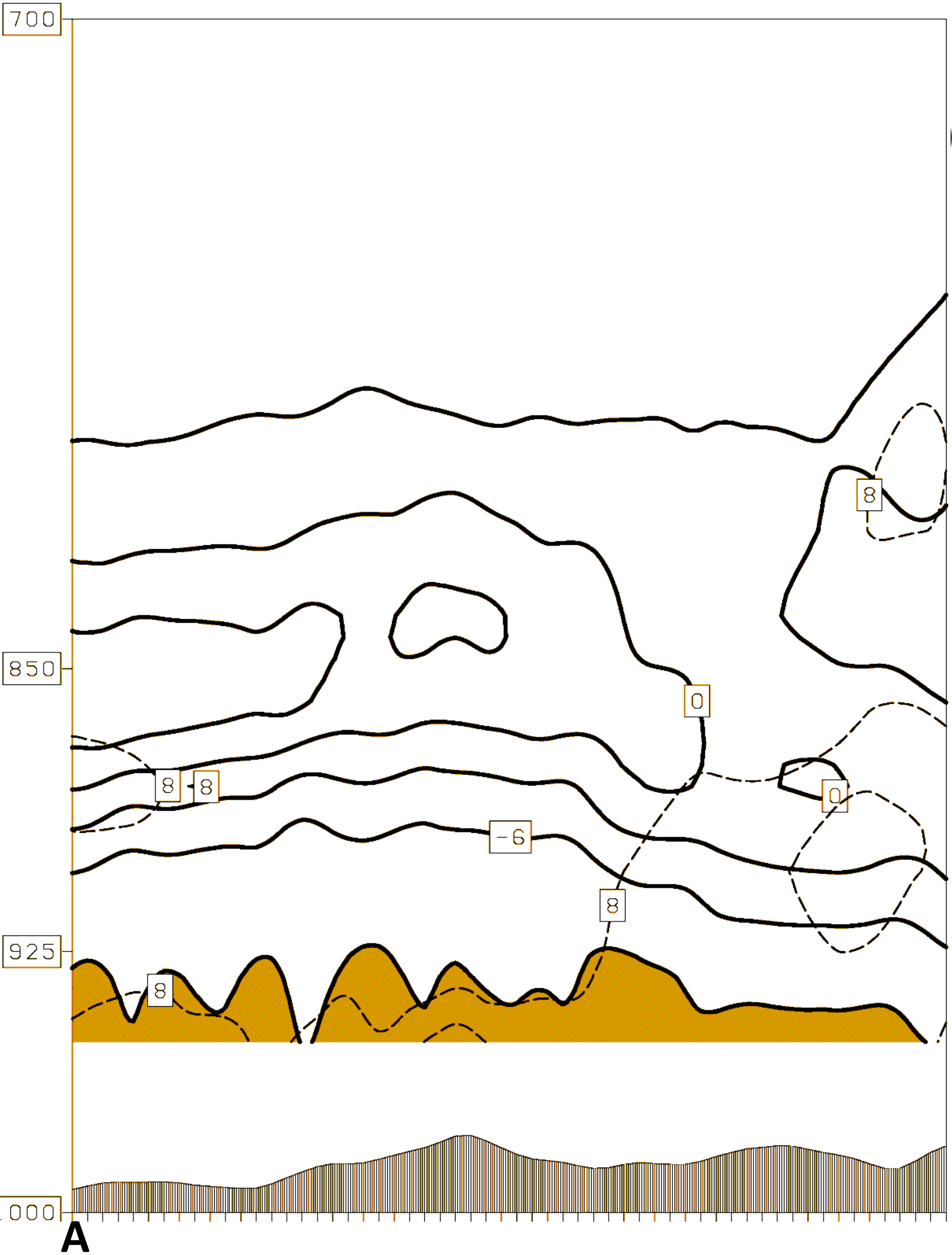

B

Model simulated environmental lapse rate (contoured in solid lines every 3°C km^{-1}) and wind shear (contoured in dashed lines; 8 and 12 x 10^{-3} s^{-1}) with steep lapse rates (magnitude exceeding 9°C km^{-1}) shaded valid at 1800 UTC 6 December [F18] for the <u>zero surface SH flux</u> experiment. Section is located in Kentucky.

Upstream of Cumberland Plateau

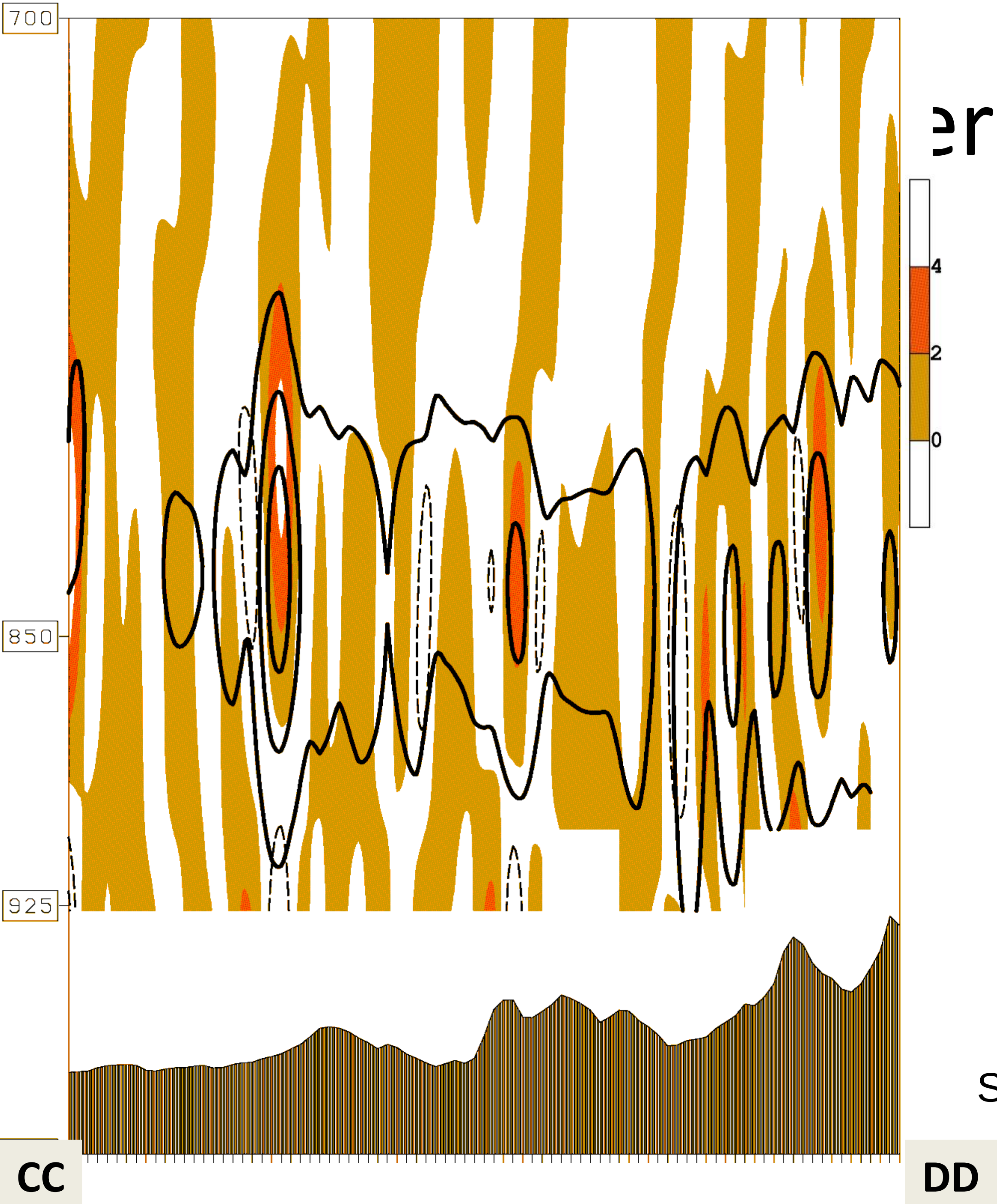

eriments

Model simulated cloud mixing ratio (contoured in thick solid lines; 1, 5, 10, and 15 x 10^{-2} g kg^{-1}) and divergence of cross-band winds (convergence contoured in dashed lines; -2, -4, and -6 x 10^{-4} s^{-1}, divergence is shaded) valid at 2100 UTC 6 December [F21] for the <u>enhanced surface SH flux</u> experiment.

Section in the Tennessee Valley

eriments

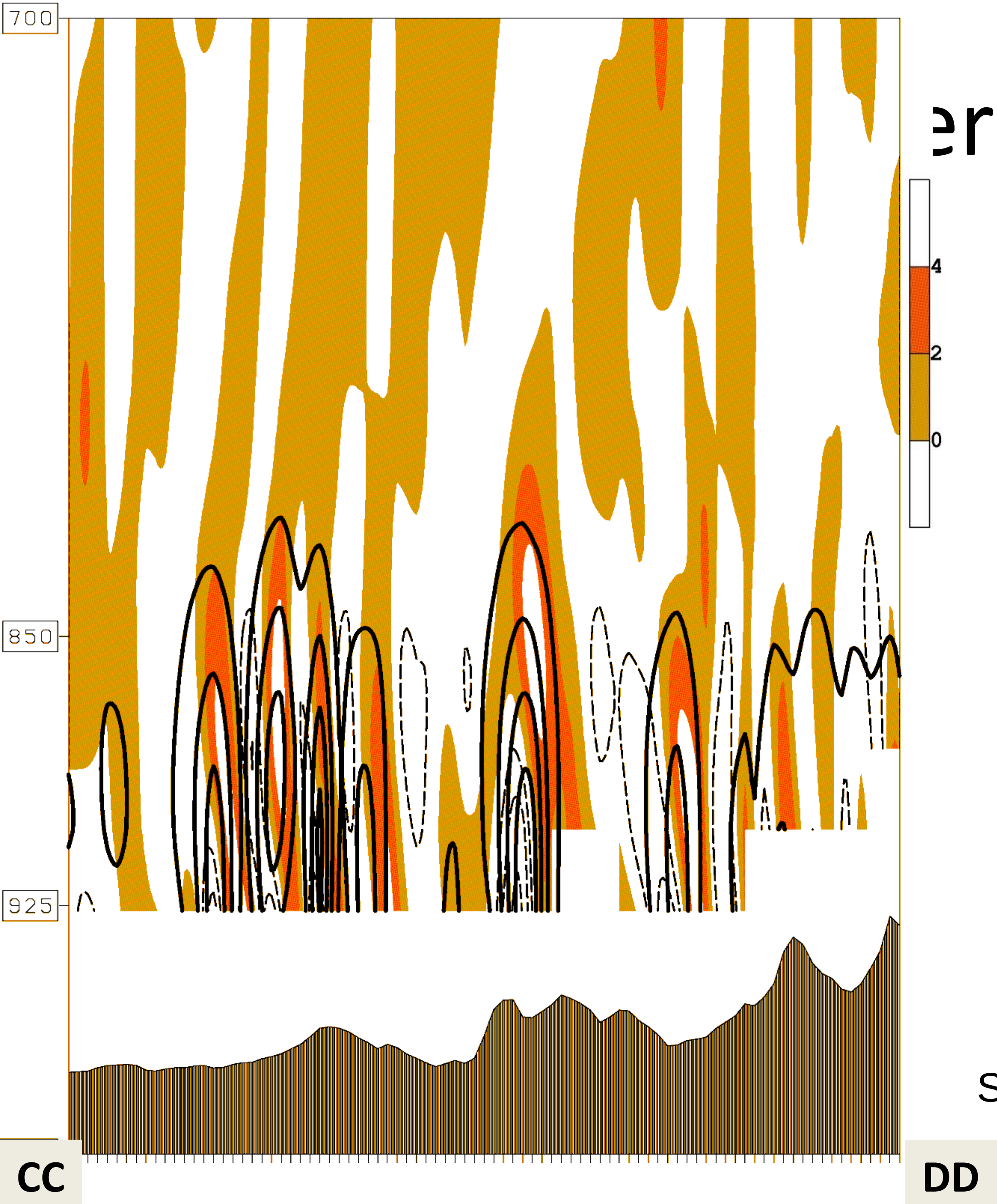

Model simulated cloud mixing ratio (contoured in thick solid lines; 1, 5, 10, and 15 x 10^{-2} g kg^{-1}) and divergence of cross-band winds (convergence contoured in dashed lines; -2, -4, and -6 x 10^{-4} s^{-1}, divergence is shaded) valid at 2100 UTC 6 December [F21] for the zero surface SH flux experiment.

Section in the Tennessee Valley

WRF Default Simulation

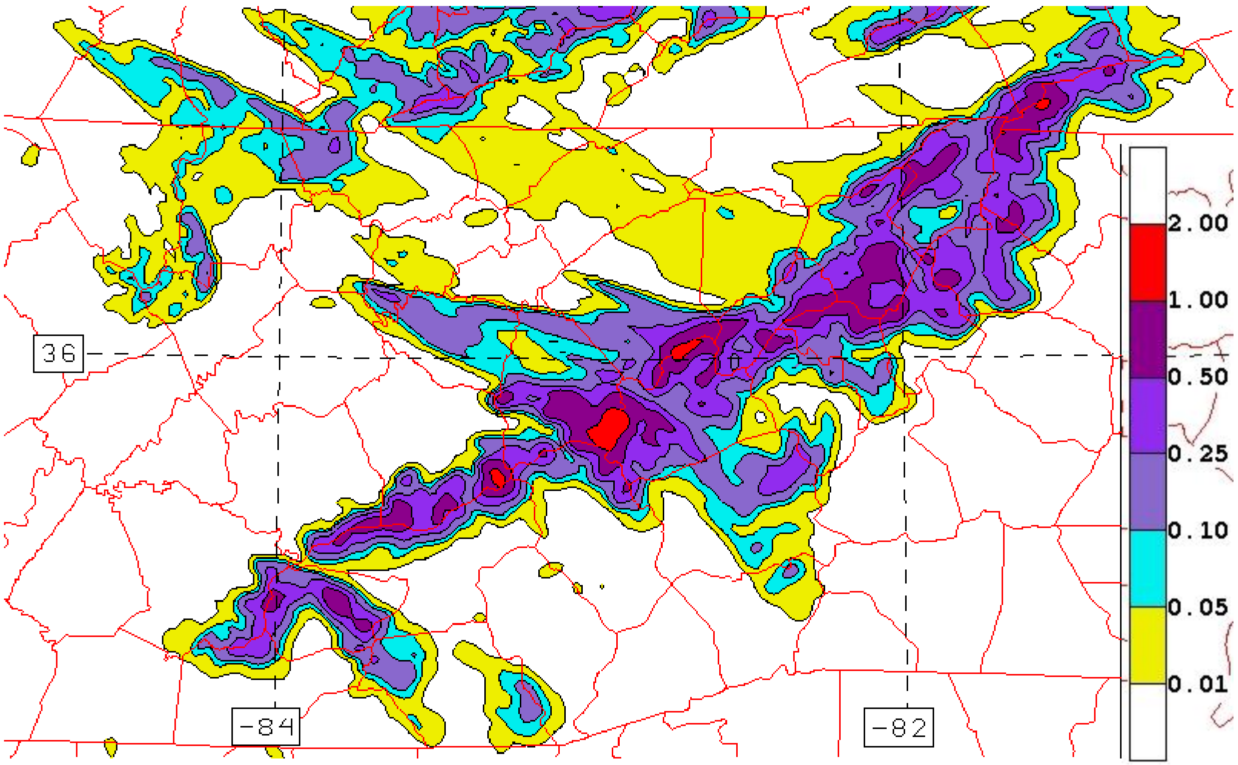

Model simulated 24-h liquid equivalent accumulated precipitation (cm) for the period ending 0000 UTC 8 December 2010 [period designated 'P34'] for the experiment having the default SH flux parameterization scheme "on" during the entire model simulation.

WRF LHF experiments

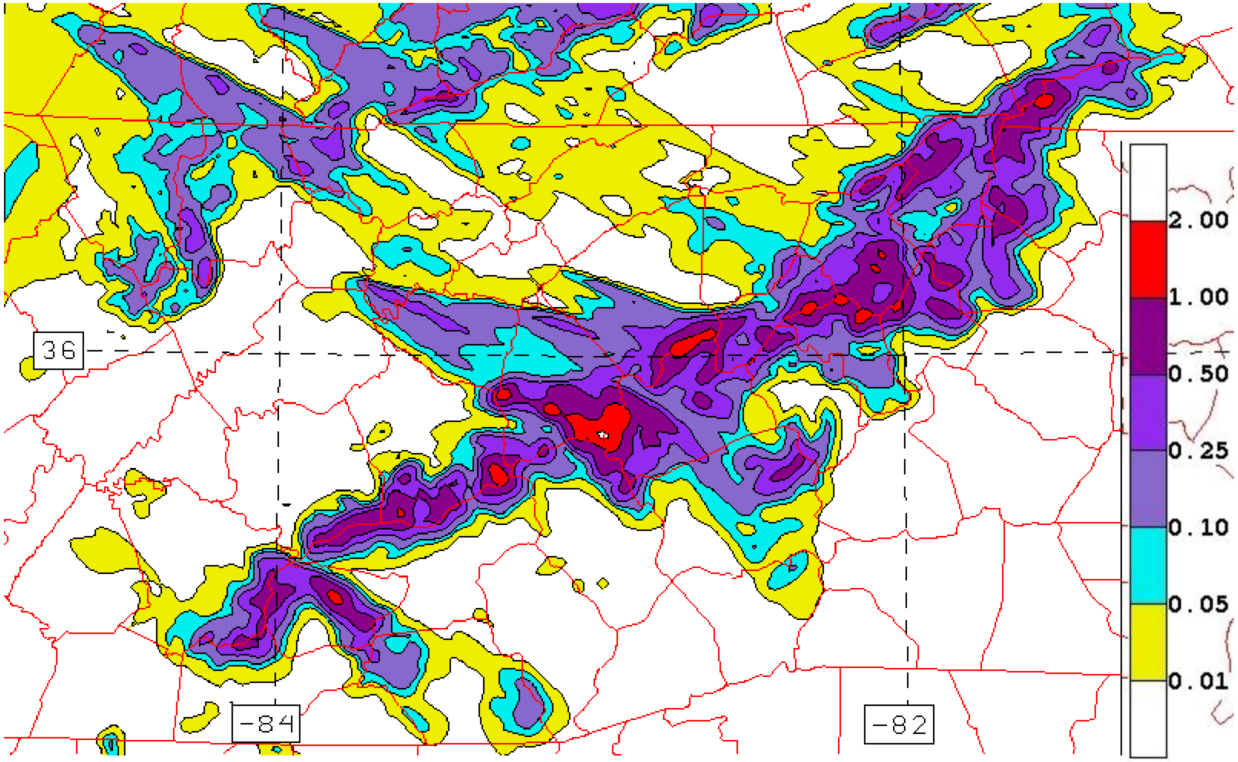

Model simulated 24-h liquid equivalent accumulated precipitation (cm) for the period ending 0000 UTC 8 December 2010 [period designated 'P34'] for the experiment having the enhanced LH flux parameterization scheme "on" during the entire model simulation.

WRF LHF experiments

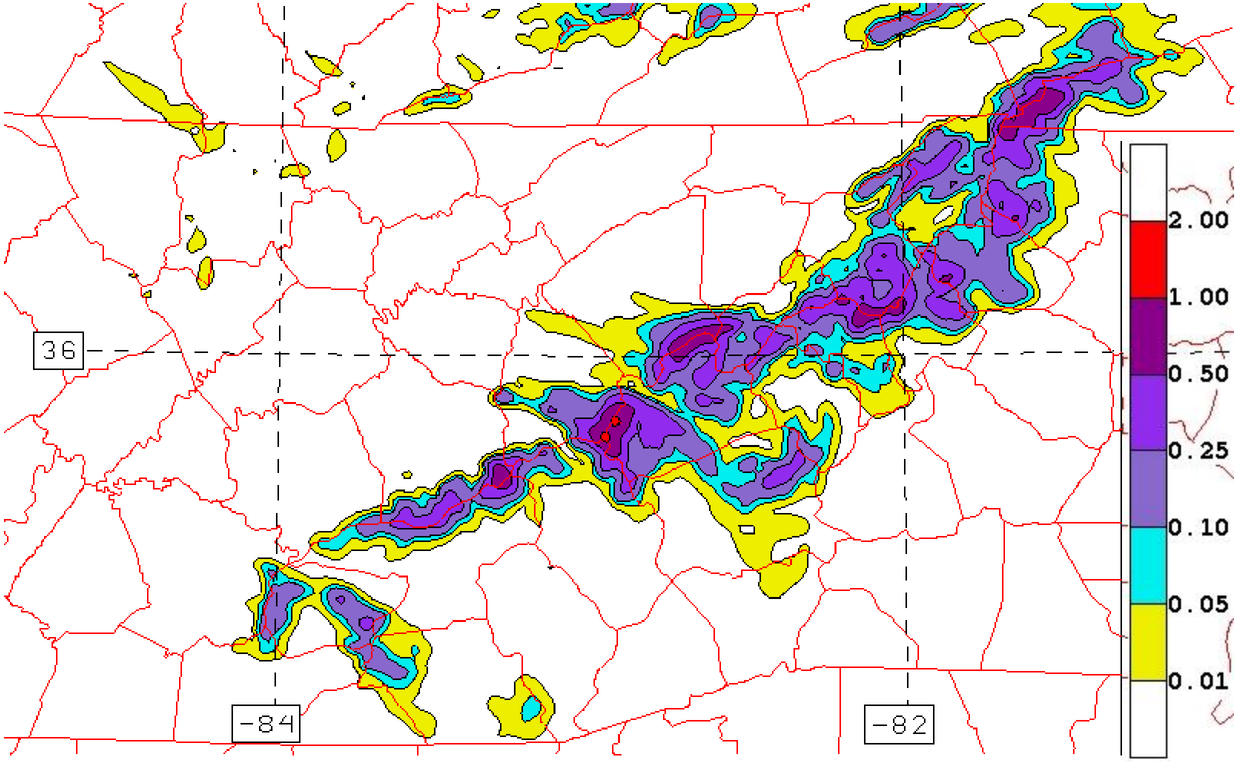

Model simulated 24-h liquid equivalent accumulated precipitation (cm) for the period ending 0000 UTC 8 December 2010 [period designated 'P34'] for the experiment having the default LH flux parameterization scheme "off" during P2.

WRF LHF experiments

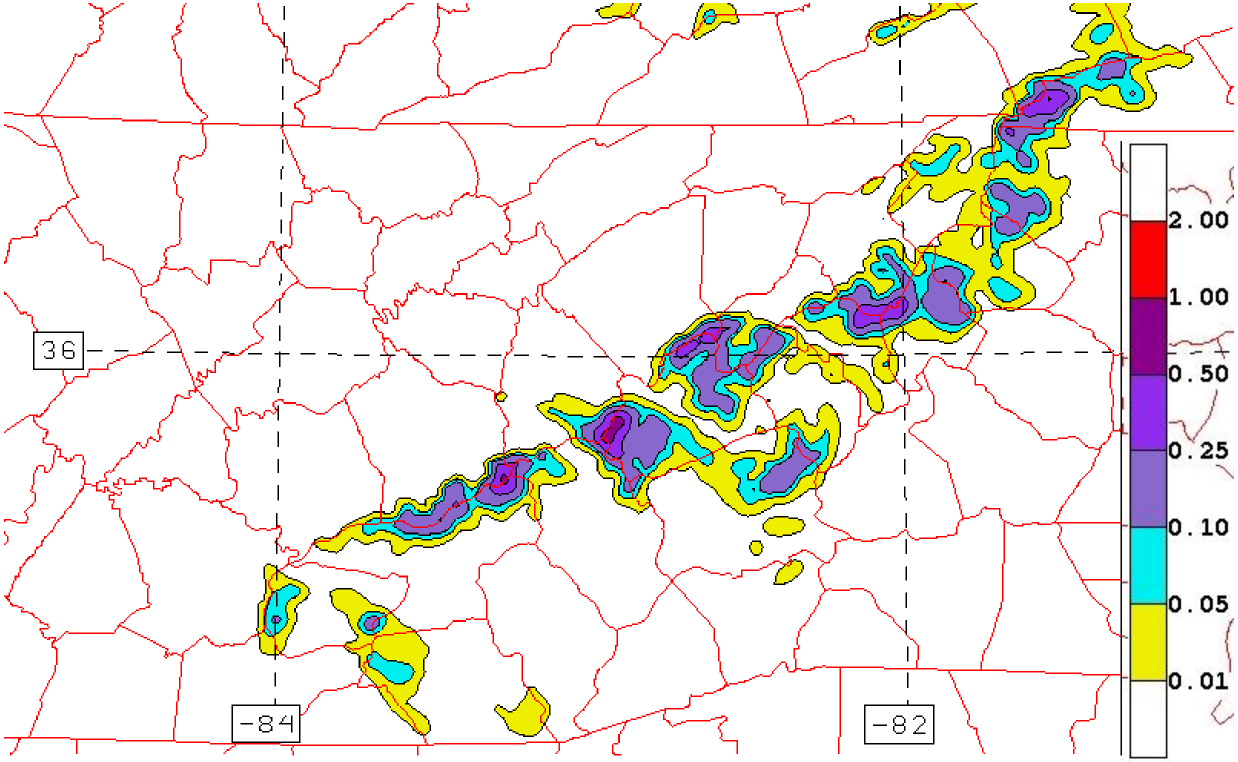

Model simulated 24-h liquid equivalent accumulated precipitation (cm) for the period ending 0000 UTC 8 December 2010 [period designated 'P34'] for the experiment having the LH fluxes shut "off" during the entire model simulation.

WRF LHF experiments

Model simulated 24-h liquid equivalent accumulated precipitation (cm) statistics

Surface LH flux parameterization	**LH scheme “off”**	**Exp. mean (cm)**	**“on” mean (cm)**	**Exp. σ (cm)**	**“on” σ (cm)**	**RMSE (cm)**	**Bias (cm)**	**N**
default	P1	0.174	0.189	0.197	0.204	0.023	-0.015	10488
default	P2	0.082	0.190	0.131	0.204	0.149	-0.109	10415
default	P34	0.157	0.190	0.182	0.204	0.048	-0.033	10421
50% enhancement	P1	0.197	0.207	0.222	0.227	0.027	-0.009	12473
50% enhancement	P2	0.112	0.238	0.164	0.236	0.171	-0.125	10419
50% enhancement	P34	0.178	0.220	0.194	0.231	0.064	-0.042	11559
N/A	ALL	0.028	0.190/ 0.238	0.060	0.204/ 0.236	0.232/ 0.290	-0.163/ -0.210	10415

Only default and experiment grid points having at least one simulation whose 24-h liquid equivalent accumulated precipitation amount exceeding 0.025 cm are included in the statistics.

Summary and forecasting implications

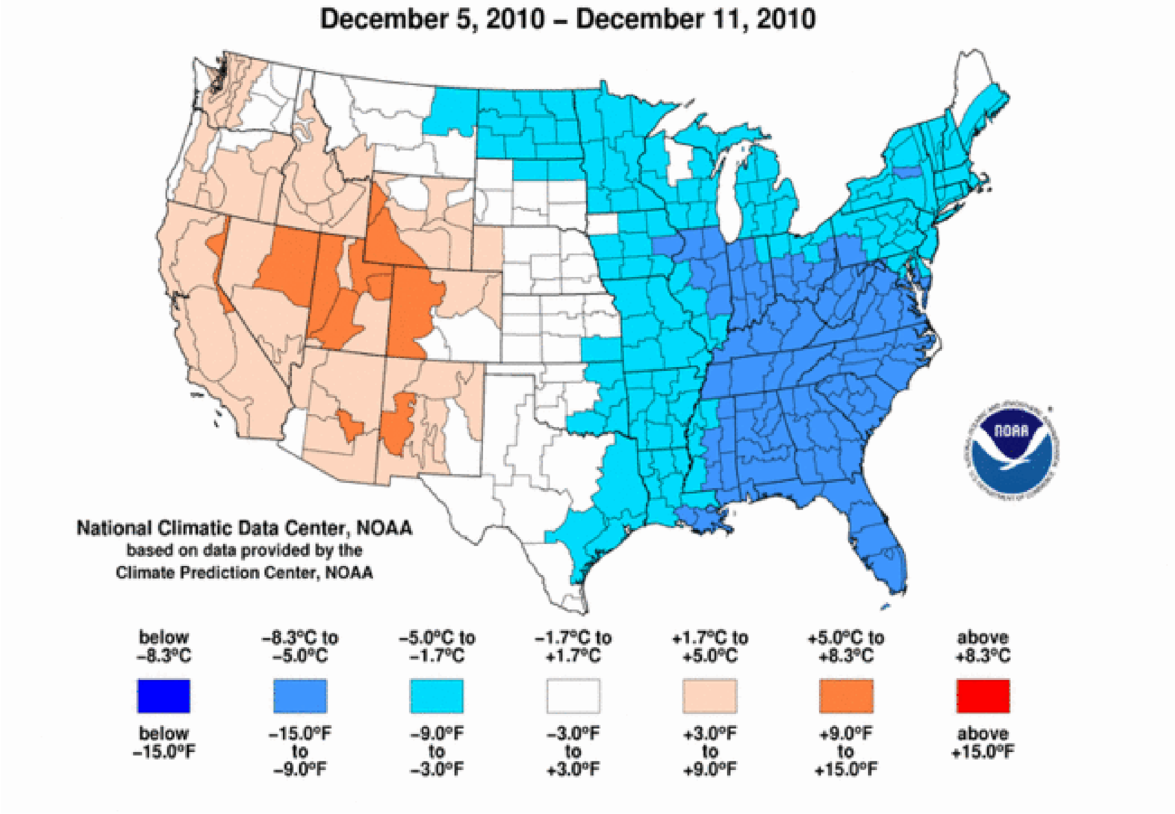

http://www1.ncdc.noaa.gov/pub/data/cmb/images/weekly/us/2010/tanom20101211-pg.gif

Summary and forecasting implications

- 6 – 8 December 2010 NWFS
  - Cancellation of classes and events on 7 December
  - Surface fluxes potentially play an important role
    - early in winter season
    - heavy rainfall event 30 Nov, 1 Dec

Summary and forecasting implications

- Numerical ***simulations*** of the ***single*** event suggest
  - Surface latent heat fluxes
    - Moisture converted to accumulated snow came from the ground over the study domain
    - Trajectory analyses indicated most of the vapor was made available in the PBL during daytime hours

Summary and forecasting implications

- Numerical ***simulations*** of the ***single*** event suggest
  - Surface sensible heat fluxes
    - Daytime fluxes oppose cloud/snow development through resultant heating and thickening of PBL
    - Daytime fluxes contribute to cloud/snow development through more efficient transport of moisture from the ground (buoyancy-driven mixing), moistening air parcels in the PBL

Summary and forecasting implications

- Forecast implications
  - Evolution of PBL temperature, moisture, depth, wind profile, and stability
    - determine production of clouds and precipitation at the top of the PBL during NWFS events
  - Cloud and snow production is suppressed if PBL is too warm, too dry, too thin, or too deep

Summary and forecasting implications

- Forecast implications
  - Optimal PBL conditions for maximizing snow production during NWFS event
    - Cool PBL that quickly becomes saturated when vapor is added via upward latent heat fluxes
    - PBL mixing of moderate strength for efficient moistening of the PBL
    - Strongest unidirectional vertical wind shear and dry adiabatic environmental lapse rate collocated next to the ground

Summary and forecasting implications

- Forecast implications
  - Optimal PBL conditions for maximizing snow production during NWFS event
    - Produces intense (deep) longitudinal cloud bands that increases the likelihood of significant snowfall accumulation downstream of the crest of the mountains
  - Optimal PBL conditions are most likely to occur during nighttime, early morning, and late afternoon hours

End of presentation

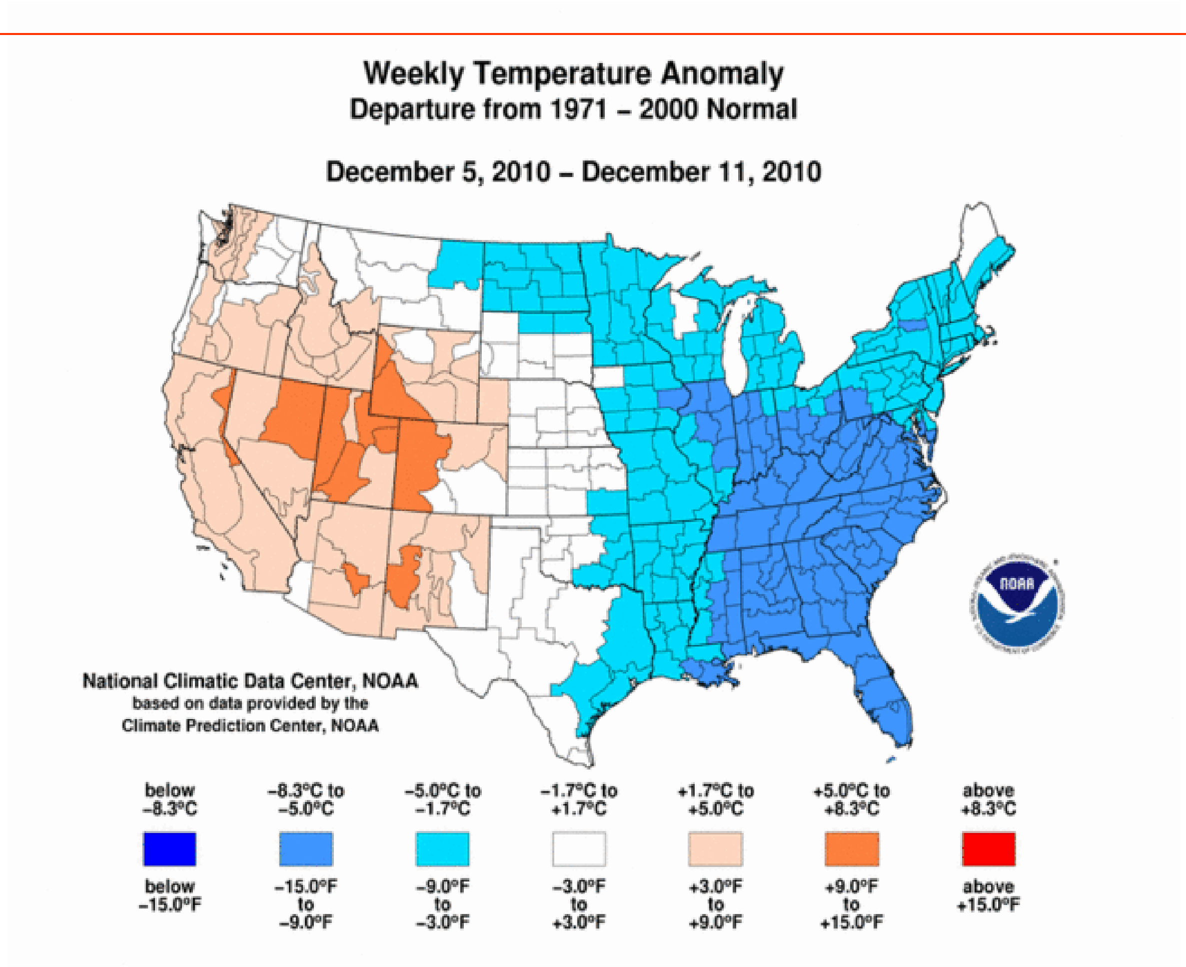

http://www1.ncdc.noaa.gov/pub/data/cmb/images/weekly/us/2010/tanom20101211-pg.gif

Extra slides

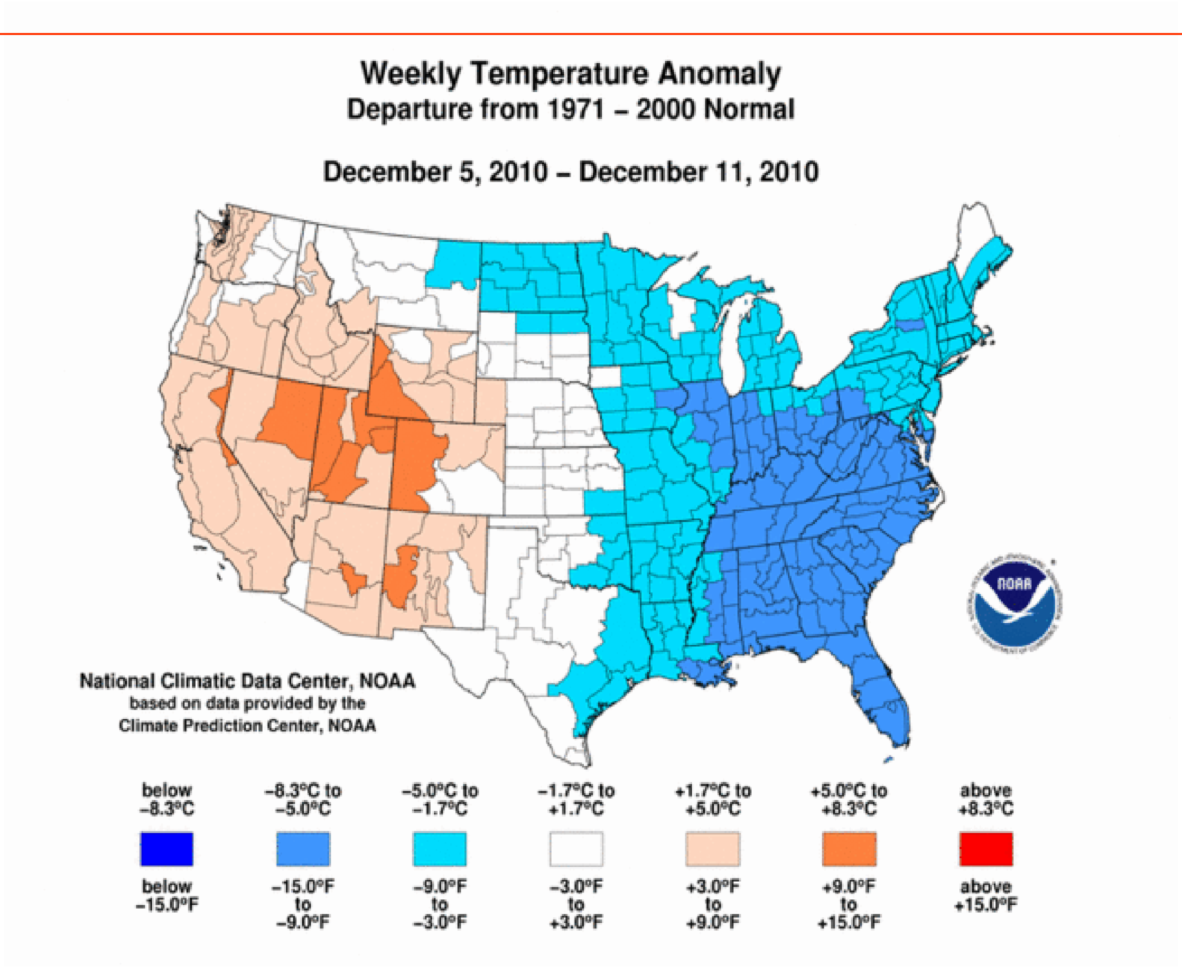

http://www1.ncdc.noaa.gov/pub/data/cmb/images/weekly/us/2010/tanom20101211-pg.gif

Methodology

- ARW-WRF model experiments
  - original ("default") and modified versions of the unified Noah land-surface model having zero surface sensible heat or latent heat, or enhanced surface sensible heat ("50% SH enhancement") or latent heat ("50% LH enhancement") fluxes during specific periods.

Summary and forecasting implications

- Numerical ***simulations*** of the ***single*** event suggest
  - Unidirectional vertical wind shear
    - Source of constant mixing in the PBL, independent of the time of day
    - Provides enough mixing to sufficiently moisten air parcels in the PBL, resulting in significant snowfall accumulations

Summary and forecasting implications

- Numerical ***simulations*** of the ***single*** event suggest
  - Surface sensible heat fluxes "off" during daytime
    - Similar total water mass as the default simulation is deposited over a broader area (increase in accumulation over the Cumberland Plateau)
      - change in precipitation banding intensity

Summary and forecasting implications

- Numerical ***simulations*** of the ***single*** event suggest
  - Precipitation banding intensity sensitive to the strength and vertical location of the layers of
    - Strongest unidirectional vertical wind shear
    - Weakest (dry adiabatic?) environmental lapse rate
      - Collocated upstream of the mountains next to the ground; precipitation banding intensity is strongest (maxima in cloud mixing ratio and magnitude of cross-band convergence)

Summary and forecasting implications

- Numerical ***simulations*** of the ***single*** event suggest
  - Precipitation banding intensity
    - Daytime buoyancy-driven mixing “lifts” layer of strongest unidirectional vertical wind shear to the inversion layer capping the PBL
    - In general, a deeper PBL minimizes the overlap of the layers of strongest unidirectional vertical wind shear and weakest stratification

    → weakened banding intensity

Summary and forecasting implications

- Numerical ***simulations*** of the ***single*** event suggest
  - Precipitation banding evolution and propagation
    - Closely tied initially to 500 hPa level cyclonic vorticity maximum
    - Intensifies and becomes locked with underlying terrain after vorticity maximum departs from study area, during the midnight hours of 7 December (0300 UTC)

References

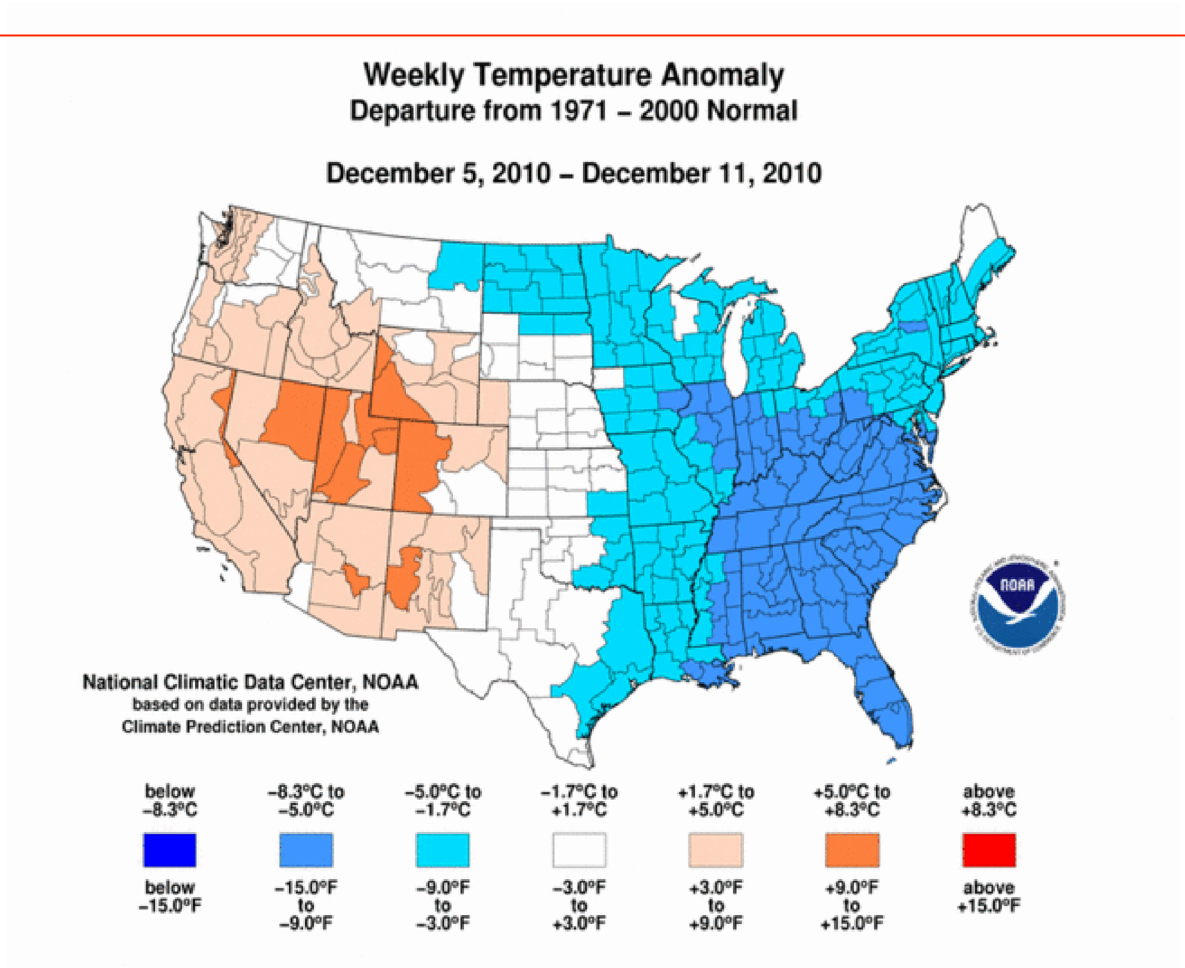

http://www1.ncdc.noaa.gov/pub/data/cmb/images/weekly/us/2010/tanom20101211-pg.gif

References

- Bergeron, T., 1965: On the low-level redistribution of atmospheric water caused by orography. Paper presented at the International Conference on Cloud Physics, Int. Assoc. of Meteorol. and Atmos. Phys., Tokyo.
- Brown, R.A., 1980: Longitudinal instabilities and secondary flows in the planetary boundary layer: A review. *Rev. Geophys. Space Phys.,* **18**, 683-697.
- Draxler, R.R., and G.D. Hess, 1998: An overview of the HYSPLIT_4 modeling system for trajectories, dispersion, and deposition. *Aust. Meteor. Mag.,* **47,** 295–308.
- -----, B. Stunder, G.D. Rolph, and A. Taylor, 2007: HYSPLIT4 user's guide. [Available online at http://www.arl.noaa.gov/documents/reports/hysplit_user_guide.pdf]
- Durran, D.R., 1986: Mountain waves. Mesoscale Meteorology and Forecasting, American Meteorological Society, P.S. Ray, Editor, 472-492.
- Fukuta, N., and T. Takahashi, 1999: The growth of atmospheric ice crystals: a summary of findings in vertical supercooled cloud tunnel studies. *J. Atmos. Sci.*, **56**, 1963-1979.
- Geerts, B., and Q. Miao, 2010: Orographic precipitation enhancement by boundary-layer turbulence: evidence from vertically pointing airborne cloud radar data. *19th AMS Conf. on Boundary Layer Processes and Turbulence*, Keystone CO, 2-6 August.

References

- Holloway, B.S., 2007: The role of the Great Lakes in northwest flow snowfall events in the southern Appalachian Mountains. M.S. thesis, Dept. of Marine, Earth, and Atmospheric Sciences, North Carolina State University, 204 pp. [Available online at http://www.lib.ncsu.edu/theses/available/etd-11022007-181739/]
- Hong, S.-Y., J. Dudhia, and S.-H. Chen, 2004: A revised approach to ice microphysical processes for the bulk parameterization of clouds and precipitation. *Mon. Wea. Rev.*, **132**, 103-120.
- Hong, S.-Y., and J.-O.J. Lim, 2006: The WRF single-moment 6-class microphysics scheme (WSM6), *J. Korean Meteor. Soc.*, **42**, 129-151.
- Hong, S.-Y., Y. Noh, and J. Dudhia, 2006: A new vertical diffusion package with an explicit treatment of entrainment processes. *Mon. Wea. Rev.*, **134**, 2318-2341.
- Hudgins, J., 2008: Mesoscale snowbands persisting downstream of the southern Appalachians during northwest flow upslope events. *33rd National Weather Association Annual Meeting*, Louisville, KY.
- Janjic, Z.I., 1994: The step-mountain eta coordinate model: further developments of the convection, viscous sublayer and turbulence closure schemes. *Mon. Wea. Rev.*, **122**, 927-945.
- Janjic, Z.I., 2000: Comments on “Development and Evaluation of a Convection Scheme for Use in Climate Models.” *J. Atmos. Sci.,* **57**, p. 3686.

References

- Kalnay, E., and Co-authors, 1996: The NCEP/NCARR 40-Year Reanalysis Project. *Bull. Amer. Meteor. Soc.*, **77**, 437-471.
- Keighton, S., L. Lee, B. Holloway**,** D. Hotz, S. Zubrick, J. Hovis, G. Votaw, L. B. Perry, G. Lackmann, S. E. Yuter, C. Konrad, D. Miller, and B. Etherton, 2009: A collaborative approach to study northwest flow snow in the southern Appalachians. *Bull. Amer. Meteor. Soc.*, **90**, 979-991.
- Kirshbaum, D.J., and D.R. Durran, 2005a: Observations and modeling of banded orographic convection. *J. Atmos. Sci.,* **62**, 1463-1479.
- -----, and -----, 2005b: Atmospheric factors governing banded orographic convection. *J. Atmos. Sci.,* **62**, 3758-3774.
- -----, G.H. Bryan, R. Rotunno, and D.R. Durran, 2007a: The triggering of orographic rainbands by small-scale topography. *J. Atmos. Sci.,* **64**, 1530-1549.
- -----, R. Rotunno, and G.H. Bryan, 2007b: The spacing of orographic rainbands triggered by small-scale topography. *J. Atmos. Sci.,* **64**, 4222-4245.
- Lackmann, G.M., 2001: Analysis of a surprise western New York snowstorm. *Wea. Forecasting*, **16**, 99-116.

References

- Mlawer, E.J., S.J. Taubman, P.D. Brown, M.J. Iacono, and S.A. Clough, 1997: Radiative transfer for inhomogeneous atmosphere: RRTM, a validated correlated-k model for the longwave. *J. Geophys. Res.*, **102** (D14), 16663-16682.
- NCDC, 2010a: *Storm Data*. Vol. 52, No. 11, 166 pp.
- NCDC, 2010b: *Storm Data*. Vol. 52, No. 12, 242 pp.
- Perry, L.B., 2006: Synoptic climatology of northwest flow snowfall in the southern Appalachians, PhD dissertation, University of North Carolina at Chapel Hill. [Available online at http://dc.lib.unc.edu/u?/etd,165]
- Perry, L.B., and Konrad, C.E., 2006: Relationships between NW flow snowfall and topography in the Southern Appalachians, USA, *Clim. Res.*, **32**, 35-47.
- Perry, L.B., C.E. Konrad, and T.W. Schmidlin, 2007: Antecedent upstream air trajectories associated with northwest flow snowfall in the southern Appalachians, USA. *Wea. Forecasting*, **22**, 334-352.
- Perry, L.B., D.K. Miller, S.E. Yuter, L.G. Lee, and S.J. Keighton, 2008: Atmospheric influences on new snowfall density in the southern Appalachian Mountains, USA. *Proceedings of the 65th Eastern Snow Conference*, Fairlee (Lake Morey), Vermont. [Available online at http://www.easternsnow.org/proceedings/2008/perry_et_al.pdf]

References

- Perry, L.B., C.E. Konrad, D. Hotz, and L.G. Lee, 2010: Synoptic classification of snowfall events in the Great Smoky Mountains, USA. *Physical Geography*, **31**, 2, 156-171.
- Pruppacher, H.R., and J.D. Klett, 1997: *Microphysics of Clouds and Precipitation*, 2nd ed. D. Reidel, 714 pp.
- Rogers, D.C., and G. Vali, 1987: Ice crystal production by mountain surfaces. *J. of Climate and Applied Meteor.*, **26**, 1152-1168.
- Ryan, B.F., E.R. Wishart, and D.E. Shaw, 1976: The growth rates and densities of ice crystals between -3^{o}C and -21^{o}C. J. Atmos. Sci., 33, 842-850.
- Schmidlin, T.W., 1992: Does lake-effect snow extend to the mountains of West Virginia? *Proc. 49th Eastern Snow Conf.*, Oswego, NY, 145-148.
- Scorer, R., 1949: Theory of waves in the lee of mountains. *Quart. J. Roy. Meteor. Soc.*, **75**, 41-56.
- Skamarock, W.C., J.B. Klemp, J. Dudhia, D.O. Gill, D.M. Barker, M.G. Duda, X.-Y. Huang, W. Wang, and J.G. Powers, 2008: A description of the advanced research WRF version 3. NCAR Tech. Note NCAR/TN-475+STR, 88 pp. [Available online at http://www.mmm.ucar.edu/wrf/users/docs/arw_v3.pdf]

References

- Sousounis, P.J., and M.J. Fritsch, 1994: Lake-aggregate mesoscale disturbances. Part II: A case study of the effects on regional and synoptic-scale weather systems. *Bull. Amer. Meteor. Soc.*, **75**, 1793-1811.
- Sousounis, P.J., 2001: Lake Effect Storms. *Encyclopedia of Atmospheric Sciences*, Holton, J, J. Pyle, and J. Curry (editors), Academic Press, London, UK, 1104-1115.
- Steenburgh, W.J., 2003: One hundred inches in one hundred hours: Evolution of a Wasatch Mountain winter storm cycle. Wea. Forecasting, **18**, 1018-1036.
- Stull, R.B., 1988: *An Introduction to Boundary Layer Meteorology.* Kluwer Academic, 666 pp.
- Warren, S., 2010: Cold settles over Asheville, Western North Carolina. *Asheville Citizen-Times,* 8 December.
- Weckwerth, T.M., T.W. Horst, and J.W. Wilson, 1999: An observational study of the evolution of horizontal convective rolls. *Mon. Wea. Rev.,* **127**, 2160-2179.
- Yoshizaki, M., T. Kato, Y. Tanaka, H. Takayama, Y. Shoji, and H. Seko, 2000: Analytical and numerical study of the 26 June 1998 orographic rainband observed in western Kyushu, Japan. *J. Meteor. Soc. Japan,* **78**, 835-856.
- Young, G.S., D.A.R. Kristovich, M.R. Hjelmfelt, and R.C. Foster, 2002: Rolls, streets, waves, and more: A review of quasi-two-dimensional structures in the atmospheric boundary layer. *Bull. Amer. Meteor. Soc.,* **83**, 997-1001.
- Yuter, S.E., L.B. Perry, D.A. Stark, and M.T. Bryant, 2007: Storm structures and precipitation characteristics of snow events in the southern Appalachian Mountains. *12th Conference on Mesoscale Processes*, Waterville Valley, NH, American Meteorological Society.